Multi-stress interaction effects on BVOC emission fingerprints from oak and beech: A cross-investigation using Machine Learning and Positive Matrix Factorization

Biplob Dey[1,3], Toke Due Sjøgren[4], Peeyush Khare[1], Georgios I. Gkatzelis[1], Yizhen Wu[1], Sindhu Vasireddy[6], Martin Schultz[6], Alexander Knohl[3,5], Riikka Rinnan[4], Thorsten Hohaus[1], Eva Y. Pfannerstill[1,2]*

[1]Institute of Climate and Energy Systems: Troposphere (ICE-3), Forschungszentrum Jülich, Jülich, Germany
[2]Institute of Geophysics and Meteorology, University of Cologne, Cologne, Germany
[3]Bioclimatology, Faculty of Forest Sciences and Forest Ecology, University of Göttingen, Göttingen, Germany
[4]Department of Biology, Center for Volatile Interactions (VOLT), University of Copenhagen, Copenhagen, Denmark
[5]Centre of Biodiversity and Sustainable Land Use (CBL), University of Göttingen, Göttingen, Germany
[6]Jülich Supercomputing Centre, Forschungszentrum Jülich, Jülich, Germany

Correspondence to: E. Y. Pfannerstill (e.pfannerstill@fz-juelich.de)

Abstract.

Forest ecosystems are increasingly stressed through heatwaves, drought periods, and other factors such as ozone pollution or insect infestations. These stressors have a profound impact on the emissions of biogenic volatile organic compounds (BVOC) from trees, which in turn influence aerosol formation and atmospheric oxidation cycles and thus feedback on the atmospheric cleansing capacity and climate change itself. While previous studies have investigated the impacts of specific stressors on BVOC emissions, analyses of combined stress effects are rare, even though the stressors seldomly occur in isolation. This study investigates the impact of heat and ozone stress, both individually and in combination, on BVOC emissions from two ecologically significant temperate tree species: European beech (*Fagus sylvatica L.*) and English oak (*Quercus robur* L.). In a climate-controlled chamber, both tree species were subjected to heat stress (38 ± 3.3°C) and ozone stress (~120 ppb), separately and in combination. BVOC emission fluxes were measured using proton transfer reaction time-of-flight mass spectrometry, and the results were compared across pre-stress, heat, ozone, and combined heat-ozone conditions.

Heat stress elicited the strongest emission increases of isoprene, monoterpene, and green leaf volatiles in both species, while ozone suppressed the emissions of most BVOCs. Combined stress led to non-additive responses different from those in single-stress scenarios. Both machine learning and positive matrix factorization analyses were performed to identify key VOC fingerprint markers that may be applied to identify stress-impacted emissions from field data, and both methods showed good agreement. The OH reactivity of the emissions, which serves as a measure for their atmospheric chemistry and ozone formation impacts, was consistently highest under heat stress for both species. However, ozone stress led to reduced OH reactivity of emissions (by 10-18%).

Our results underscore that the study of realistic combinations of stressors is crucial to understand future BVOC emissions and indicate that BVOC emissions could alter atmospheric chemistry and feedback with air quality and climate as heatwaves and

35   pollutant-induced stress become more frequent due to climate change.

1. Introduction

The interaction between the atmosphere and forest ecosystems is crucial to understand, as it is an essential part of global biogeochemical and water cycles. A variety of atmospheric factors, including drought and increasing temperatures, can affect the integrity of the biosphere and its biodiversity (Pecl et al., 2017). However, the biosphere also has the capacity to influence

40   the atmosphere (Arneth et al., 2010) by emitting various biogenic volatile organic compounds (BVOCs) from plants or soil (Pugliese et al., 2023). Every year, the terrestrial biosphere releases around 1000 Tg of BVOCs into the atmosphere (Guenther et al., 1993; Sindelarova et al., 2014), encompassing over 30,000 identified organic compounds (Peñuelas and Llusià, 2004) with diverse chemical properties and atmospheric lifetimes. BVOCs, being highly reactive, rapidly react with oxidant gases upon emissions, with lifetimes ranging from seconds (e.g., isoprene) to several days (e.g., methanol). The primary mechanisms

45   of BVOC reactions involve the oxidation by hydroxyl radicals (OH) and ozone (O_3) (Palm et al., 2018). These processes have substantial implications for the formation of tropospheric ozone and secondary organic aerosols, subsequently influencing air quality, cloud formation and contributing to climate dynamics (Palm et al., 2018; Vella et al., 2023).

Over the past century, the global average temperature has risen by 1.5 °C (IPCC, 2023). With the recent intensification of global climate change, there has been a noticeable increase in the frequency and intensity of heatwaves worldwide

50   (Zscheischler et al., 2020). This trend is particularly pronounced in Europe (IPCC, 2023). Also, projections indicate that by 2100, the global temperature may further increase by 2–6 °C (Daussy and Staudt, 2020), and this warming will increase drought risk (Cook et al., 2018). Consequently, this phenomenon not only directly impacts plant primary productivity but also has cascading effects on biogeochemical cycling processes within terrestrial ecosystems. As temperature (Roy et al., 2024) and soil water content are key drivers of plant metabolism, this anticipated climate change scenario is expected to heighten stress

55   levels on plants (Jiang et al., 2019), leading to substantial changes in BVOC fluxes. However, the overall direction of that change is to date uncertain, complicating BVOC predictions under future climate (Szopa et al., 2021) – one of the reasons for this uncertainty being the impact of climate-induced (combined) stressors.

Tropospheric O_3 concentrations are rising globally (0.5–2.0% yearly). Climate change is also expected further to exacerbate ground-level O_3 at local and regional scales, increasing the frequency of high pollution days. Regions like Europe are likely to

60   experience more elevated O_3 events (Royal Society, 2008). As a highly phytotoxic gas, O_3 significantly affects plant growth and development, with acute exposure causing necrotic damage and chlorophyll loss in leaves (Karnosky et al., 2007). To complicate matters, the interaction between O_3 exposure and trees is reciprocal (Paoletti, 2009): trees are affected by O_3, and influence O_3 levels in the air. Forest vegetation interacts complexly in regulating local tropospheric ozone concentrations, as

trees can both scavenge and contribute to O_3 formation. The net effect depends on factors such as tree species, physiological

65 status, environmental conditions, and air chemistry (Kivimäenpää et al., 2013; Pinto et al., 2010).

Plant-released BVOCs, significantly influenced by external factors (Fitzky et al., 2019), are essential for intra- and interspecific communication (Heil and Karban, 2010), defense mechanisms against herbivores and pathogens (Dicke and Baldwin, 2010), and other biotic and abiotic interactions. These compounds primarily stem from metabolic processes from the leaf mesophyll tissues (e.g., mevalonate (MVA), methylerythritol phosphate (MEP), Lipoxygenase (LOX) or Shikimate pathway). More

70 specifically, MEP and MVA are responsible for isoprenoid production (Bergman et al., 2024), including monoterpenes (MTs) and diterpenes, which contribute to thermal tolerance, whereas the LOX pathway is integral to green leaf volatiles production in response to mechanical damage or herbivory (Kutty and Mishra, 2023). While basic patterns of BVOC emissions in response to light and temperature are reasonably well understood and parameterized (Guenther et al., 2012), a large uncertainty around BVOC emissions is caused by the impact of stress. When plants undergo stress induced by factors such as drought, heat,

75 herbivory, or elevated ozone levels, they can undergo fundamental changes in the composition and quantity of their emissions (Holopainen et al., 2018). This introduces a notable challenge in accurately predicting BVOC emissions under varying stress conditions.

Under non-stressed conditions (i.e., constitutive emissions), plants typically invest a low amount of carbon, approximately 1-2% of assimilated carbon (Fineschi et al., 2013), in BVOC emissions. However, during stress, emissions can increase

80 significantly, sometimes exceeding the use of 10% of the assimilated carbon (Niinemets et al., 2010). The response of plants to heat stress depends on the intensity of the temperature (Guenther et al., 1993). As a defensive mechanism, plants increase isoprenoid production to stabilize the cellular thylakoid membranes and protect the photosynthetic apparatus (Sharkey, 2005). Also, heat stress can induce very high emissions of isoprene and monoterpenes by enhanced biosynthesis or increased vapor pressure of stored compounds (Werner et al., 2020) that the temperature-based models for constitutive emissions cannot

85 explain (Nagalingam et al., 2023). High temperatures reduced the de novo emissions of certain BVOCs, particularly in conifers, where thermal stress amplifies the release of monoterpenes stored in resin ducts and induces the production of green leaf volatiles (Kleist et al., 2012b). Numerous studies (Bourtsoukidis et al., 2012; Fitzky et al., 2023; Genard-Zielinski et al., 2018; Kivimäenpää et al., 2013, 2016; Kleist et al., 2012b; Pikkarainen et al., 2022) have emphasized that BVOC emission rates are species-specific and depend on external meteorological factors (such as soil moisture, temperature, and CO_2 concentrations).

90 For example, higher sesquiterpene emissions were observed in Scots pine during heat stress (Kivimäenpää et al., 2016), whereas lower sesquiterpene and monoterpene emissions were found for European beech under heat stress (Kleist et al., 2012b). From the drought and heatwaves experiments of Aleppo pine, Birami et al. (2021) showed that most BVOC emissions exponentially increased during the first heat wave. However, the emissions of monoterpenes and methyl salicylate showed reduced temperature sensitivity on the second heatwave.

95 Under O_3 stress, plants reduce O_3 influx into their tissue by regulating stomatal closure, mediated by calcium ions and hormonal signals (Guo et al., 2024). As O_3 induces the formation of reactive oxygen species (ROS), plants use enzymatic defenses (e.g., catalase, superoxide dismutase) to detoxify and mitigate lipid peroxidation in cell membranes (Feng et al., 2021). Also, it can

activate the involved antioxidant enzymes gene expression (e.g., glutathione S-transferase, L-ascorbate peroxidase) (Baier et al., 2005) resulting in induced and modulated emission of BVOC. Studying Norway spruce, Kivimäenpää et al. (2013) a moderate temperature increase (~1 °C above ambient) significantly enhanced BVOC emissions, especially monoterpenes and sesquiterpenes, but this effect was partially suppressed by elevated ozone levels (~1.5× ambient). Elevated O_3 concentration (80 ppb) significantly increased the BVOC (mainly isoprene) emission rate of Chinese red pine (Xu et al., 2012). Moreover, Peron et al. (2021) found that isoprene emissions decreased while monoterpene and sesquiterpene emissions increased under combined drought and ozone stress in Oak. But under drought stress (without O_3), Fitzky et al. (2023) identified slightly elevated monoterpene and isoprene emissions from beech and oak.

The overall impact of stress-induced changes in BVOC emissions remains elusive, specifically under multiple stressors (Yang et al., 2025), as the effect of blending two stressors, like heat + O_3 or O_3 + elevated CO_2 is not well-understood (Holopainen et al., 2018), and responses may vary between species. When multiple stresses are induced at the same time, their effects on plant emissions can be additive, subtractive, or one of them may have a dominant impact. Our study specifically aimed (1) to investigate BVOC emission flux patterns from both tree species under heat or ozone and combined stress in controlled environmental conditions, (2) to identify specific stress marker BVOCs for beech and oak for the identification of stress-induced BVOC emissions in future field measurements, (3) to estimate the potential atmospheric impact of changing emission patterns in terms of OH reactivity as an indicator for ozone formation potential.

2. Materials and methods

2.1 Experimental set-up

2.1.1 Plant chamber and stress treatment

The experiment was carried out in the interlaced atmosphere simulation chamber SAPHIR (Simulation of Atmospheric PHotochemistry In a large Reaction Chamber) and PLUS (Plant Chamber Unit for Simulation) at the Forschungszentrum Jülich, Germany, during the summer, 2024. However, this study only analyzed measurements obtained directly from the PLUS chamber (Fig. 1a). The PLUS plant container is a custom-build, gas-tight, temperature- and light-controlled container that can house up to six tree-type plants. Inside the chamber, a rectangular aluminum frame supports a 9.32 m^3 Teflon film enclosure containing the upper portions of potted trees. This enclosure separates the soil from the stems and the leaves of the trees. PLUS operates in a dynamic flow-through mode using a turbulent airflow of 100 lmin^{-1} of synthetic air that passes through the Teflon enclosure, ensuring homogeneous, steady-state conditions inside the chamber. Important environmental factors within the PLUS chamber, such as temperature, photosynthetically active radiation (ranging from 0 to 800 µmol m^{-2} s^{-1} at a distance of one meter), and soil moisture, were controlled (Hohaus et al., 2016). After installation of the experimental saplings, the PLUS Teflon enclosure was kept at a slight overpressure of approximately 35 Pa to prevent any trace gases from diffusing into the

enclosure. The synthetic air was mixed with 400 ppm CO_2 to maintain levels necessary for plant photosynthesis. More details about the functional and structural description can be found in Hohaus et al. (2016).
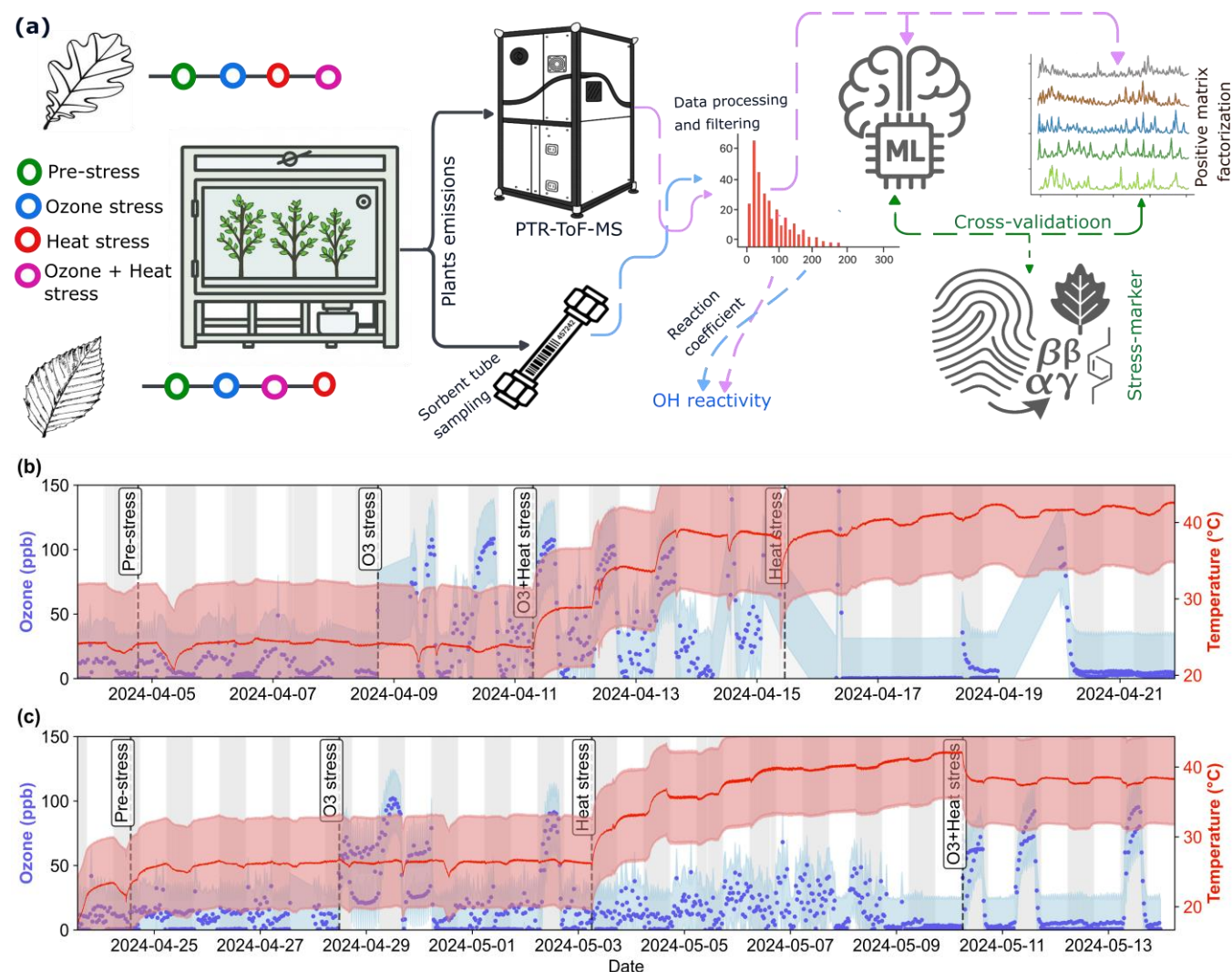
Figure 1. Overview of experimental design and stress timeline for beech and oak. (a) Schematic illustration of the experimental setup, data processing and analysis pipeline, (b, c) time series of ozone concentration (blue) and temperature (red) during pre-stress and stress phases for beech (b) and oak (c). The experiment is divided into four consecutive phases: Pre-stress, O₃ stress, Heat stress, and O₃+Heat stress, indicated by vertical dashed lines. White and grey background areas represent day and night periods, respectively. Shaded regions around lines represent the standard deviation from the mean ozone concentration and temperature.

Experiments were conducted with two major forest tree species in Germany: *Quercus robur* L. (English oak) and *Fagus sylvatica* L. (European beech). Before the experiment, 24 saplings of ~1.4 m in height of beech (12 individuals) and oaks (12 individuals) were selected under conditions ensuring they were disease-free, had straight stems, and were overall healthy. The plants were kept in a greenhouse under near-ambient light conditions with photosynthetically active radiation. During this period, they were watered regularly. To quantify the total leaf area of each plant, all leaves were photographed against solid

blue backgrounds at known distances and scales right before installing them in the plant chamber. Four images were taken from different angles for each individual to reduce bias. Then we processed these images using the ImageJ software according to Schneider et al. (2012), to extract the leaf area, and estimated total leaf area using the geometric means.

The first experiment was conducted with beech trees from April 3, 2024, to April 23, 2024 (Fig. 1b). Six trees were selected

145 from the 12 available and placed into the plant chamber. Stems were sealed with Teflon foil to isolate the canopy from the soil. One beech branch had to be cut for the tree to fit into the chamber, potentially impacting emissions in the first days of the experiment. The first 24 hours after setting up the experiment were considered the plant adaptive period, and data from this period were excluded from the analysis. Oak experiments were conducted in a similar fashion from April 24, 2024, to May 13, 2024, using the six healthiest individuals (Fig. 1c).

150 Following the pre-stress period, ozone, ozone + heat, and solely heat stress were periodically induced on the beech trees. For heat stress experiments, temperature was gradually increased (Fig.1b, c) and ozone was (except for two days for the oak experiment, Fig. 1c) applied during the night cycle. This approach avoided reactions of emitted terpenoids with ozone during the day, when emissions are highest, which would interfere with quantifying primary BVOC emissions because it would produce oxygenated VOC products. For later analysis of BVOC emissions we excluded data from nights and from the two

155 days where ozone was applied, to avoid ozone impacts on the observed VOCs.

The ozone concentration in both experiments ranged from 0 to 120 ppb. During ozone stress and ozone + heat stress, ozone concentrations were 90 ± 21.5 ppb and 93.1 ± 19.6 ppb, respectively. Soil moisture was maintained at 50-80% (relative sensor readings) with air temperatures ranging from 20 °C to 44 °C. When no heat stress was applied, air temperature was 25.9 °C ($\pm$ 0.6°C). During heat stress and combined stress, it was 38 ± 3.3 °C and 38.1 ± 0.4°C, respectively. Light conditions remained

160 constant during the day (UTC (coordinated universal time) 16:00–6:00), with lights turned off at night (UTC 6:00-16:00). At the end of the experiments (after ozone + heat stress), the plants had wilted.

2.1.2 VOC emission measurements: PTR-ToF-MS

Air was sampled from the SAPHIR-PLUS chamber through a thermally insulated and heated 1/4'' PFA line with a flow rate of ~3 lmin^{-1}. Real-time BVOC signals were measured using a proton transfer reaction time-of-flight mass spectrometer (Vocus

165 PTR-ToF-MS, Krechmer et al. (2018)) with a 1-second time resolution. The PTR-ToF-MS was operated with a drift tube temperature of 100 °C, a drift voltage of 600 V, and a drift pressure of 2.5 mbar in proton transfer ionization (H_3O^+) mode. Mass resolution of the instrument was around 8000.

A gas standard mixture containing 19 compounds with masses ranging from 33 amu (atomic mass unit) to 671 amu (Table S1, in supporting information), that was calibrated against a gravimetrically prepared, certified standard, was used for regular

170 calibrations. PTR-ToF-MS data was processed using Tofware. A mass list was prepared with 500 compounds for both experiments from a mass-to-charge ratio (m/z) range of 18 amu to 450 amu (details in supplementary data, sheet "Identity_mz"). Zero air measurements were conducted hourly and used for background subtraction.

Sensitivities for compounds not included in the gas standard were estimated using a theoretical calibration method according to Cappellin et al. (2012). This involved fitting a sigmoidal function, which reflects the expected transmission characteristics
175   of a Vocus-PTR-ToF-MS after dead time correction, to the reaction-rate-normalized sensitivities of VOCs that were calibrated using the gas standard and are known to not fragment or cluster (Jensen et al., 2023; Pfannerstill et al., 2023). Emission fluxes were calculated from such derived concentrations using the chamber flow rate and the leaf area (Edtbauer et al., 2021).

To ensure quality and reliability, flux data were filtered using a systematic signal-to-noise ratio (SNR) approach. For each compound, the SNR was calculated as the ratio of its measured flux to its corresponding LOD value at each time point.
180   Compounds were selected whose SNR was greater than or equal to 3 for at least 30% of the time series. Compounds that did not meet both the SNR threshold and the minimum temporal coverage requirement were excluded from further analysis. Applying the SNR threshold, 80 and 82 VOC species for beech and oaks were selected, respectively. The uncertainties in both the theoretical and gas-standard calibrations were assessed based on average estimates. For the theoretical calibration, the uncertainty was estimated at 51.3%, while the gas-standard calibration uncertainty, consisting of the calibration standard
185   uncertainty and the mass flow controller uncertainty, was estimated at 10%.

Exact masses and attributed chemical formulas are reported. Attribution of compound names to chemical formulas was performed to the best of our knowledge, however, identification is tentative because the PTR method cannot distinguish isomers and is subject to fragmentation.

2.1.3 Terpenoid composition: GC-MS

190   The PTR-ToF-MS method (Section 2.1.2) identifies exact masses of compounds which can be attributed to a chemical formula but cannot separate isomers. Structural identification of mono- and sesquiterpenes was performed by sampling onto stainless steel tubes (Markes International Limited, England) packed with Tenax TA (porous organic polymer) and Carbograph 1TD (graphitized carbon black) sorbents.

Sorbent tube sampling was performed with a modified MTS-32 autosampler (Markes International Limited, England), which
195   was directly connected to the PLUS via a PFA line. The autosampler consists of a stainless steel manifold block, timer, mass flow controller, vacuum pump (Laboport N86 KT.18, KNF, France), and a copper ozone scrubber treated with potassium iodide. Sorbent tubes were fitted with diffusion locking caps (Markes International Limited) to prevent contamination. Flow rates during sample collection varied from 50 to 300 ml min^{-1} due to technical constraints of the autosampler, with 300 ml min^{-1} occurring during the oak experiment's pre-stress and ozone exposure phases. However, this variation is not likely to affect
200   the results. After sampling, sorbent tubes were sealed with brass storage caps and stored at 4° C until analysis.

Analysis of the sorbent tubes was performed with an Agilent gas chromatograph coupled with a mass spectrometer (7890A GC—5975C inert MSD, Santa Clara, USA). Sorbent tubes were thermally desorbed at 250°C for 10 min (TD100-xr, Markes International, Llantrisant, UK) and cryofocused at 10°C, before being transferred to the GC–MS system through a capillary column at 160°C. An HP-5MS capillary column (50 m × 0.2 mm × 0.33 μm, Agilent Technologies, Santa Clara, USA) was
205   used to separate the VOCs with a carrier gas flow of 1.2 mL min^{-1} of helium. The oven program used an initial temperature of

40°C for 3 min, before ramping at 5°C min⁻¹ to 210°C, and again at 20°C min⁻¹ to 250°C, and a final hold of 8 min to give a total runtime of 47 min. The ion source and quadrupole temperatures were held at 230°C and 150°C, respectively. No-injection column blanks and empty stainless-steel cartridges (containing no sorbent material) were run periodically alongside the samples to provide an indication of background contamination arising from the analytical system (e.g., siloxanes, phthalates).

210 Travel blanks (unopened, pre-cleaned sorbent cartridges that travelled to and from the field site alongside the sample tubes) were also analysed.

Chromatograms from the GC-MS laboratory analysis were processed using the PARADISe V.6.1 software (Quintanilla-Casas et al., 2023). Compounds were identified based on pure standards and tentative identification based on matches with the NIST 2023 Mass Spectral Library (National Institute of Standards and Technology, Gaithersburg, MD, USA). Compounds with a

215 match factor above 800 and probability above 30 were accepted, as well as compounds with 3 hits of the same structural formula. Incompatible compounds were manually assessed and identified by structural formula or probable matches. Concentrations were quantified using the external standards. In the cases of unavailable standards, the closest structurally related standard compounds were used. Contaminant compounds that are known to arise from plastics, the analytical system, sorbent tubes, or personal care products were excluded from the dataset.

220 Identification of mono- and sesquiterpenes from GC-MS data was used to calculate OH reaction rates for the average isomeric composition for each experiment phase. Species-stress-specific OH reaction rate coefficients are available in supplementary data. Only daytime emission data were used to account for both de novo and stress-induced BVOC emissions.

2.2 Integrated analytical approach

BVOC emissions in response to stress are not static; they change over time as the stress persists or alleviates. Also, plants

225 might start emitting a particular compound as a response to an initial stress signal, and the concentration might increase, decrease, or change composition, with many different compounds being emitted simultaneously as the stress continues. Given this complexity, classical statistical methods are limited unless the underlying relationship between variables is understood or predefined. In contrast, advanced algorithms (e.g, machine learning, positive matrix factorization) excel in uncovering complex, nonlinear patterns without requiring explicit assumptions about variable interactions. Therefore, machine learning

230 (ML) and positive matrix factorization (PMF) were used to comprehensively analyze BVOC stress fingerprints (Fig. 1a).

A supervised ML model classified four treatment categories: pre-stress, ozone stress, heat stress, and ozone + heat stress, based on consecutive emission profiles. To interpret the model's decision-making process and identify the important features, SHapley Additive exPlanations (SHAP) were used. SHAP analysis enabled features or BVOC compound-level interpretability by indicating whether high or low emissions of individual VOCs contributed to specific stress classifications, thereby providing

235 both directionality and diagnostic specificity.

In parallel, PMF, an unsupervised source apportionment method, extracted latent emission profiles and their temporal dynamics. PMF resolved the VOC emissions into co-varying compound groups (factors) corresponding to physiological

responses (e.g., early heat stress, oxidative damage, late heat stress, etc.). PMF and ML offer complementary perspectives: PMF elucidates temporal emission patterns, whereas ML identifies the most informative features for distinguishing stress types. The comparison between results from ML and PMF thus allows for higher certainty in fingerprint identification than one single method would provide.

2.2.1 Machine learning model: Random Forest

Time-resolved VOC measurements from beech and oak experiments under four stress conditions were used to train a machine learning model for classifying stress conditions (Fig. 1). It contains 20-minute resolution daytime VOC data over the 2 months (Figs. S5a and S6a in the supporting information) containing flux of each VOC, stress label, and time. A structured preprocessing pipeline was applied to ensure the integrity of the input data and enhance model performance. First, the dataset was checked for invalid measurements in VOC flux features; no missing, null, or zero values were found. Then, variance-based filtering was applied to remove quasi-constant features to reduce redundancy and exclude non-informative VOCs. Subsequently, correlation was checked between the features (by Pearson correlation) to avoid multicollinearity. Absolute correlations greater than 90% were flagged, and features were reviewed and only retained if they were biologically and chemically justified. Subsequently, a logarithmic transformation was applied to reduce skewness, scale down extreme flux magnitudes, and improve distribution symmetry. To normalize feature scales and stable model optimization, the log-transformed data were standardized.

The dataset was split chronologically into training and test subsets for model training using a stratified temporal splitting approach (Figs.S5c and S6c). Within each stress class, 70 % of the earliest samples were allocated to the training set and 30 % to the test set. This approach ensured temporal separation between training and test periods, also a balanced representation of all classes (Figs. S5b and S6b). An alternative configuration was used as a sensitivity check in which an equal number of samples were randomly selected from each day and assigned to the training and test sets. No substantial differences in model performance were observed between the two approaches.

A random forest (RF) model was used to classify stress due to its robustness, interpretability, and ability to handle structured data. The implementation followed the scikit-learn python framework (Pedregosa et al., 2012) for machine learning. A hyperparameter optimization step was performed using grid search to tune the number of trees, maximum tree depth, minimum number of samples per split, and minimum number of samples per leaf. The optimization was carried out using 3-fold cross-validation with the weighted F1 score as the evaluation metric. Model performance was recorded across all parameter combinations, and the one with the highest validation score was selected for the final model fitting.

Robustness of the model was evaluated through a non-parametric bootstrapping procedure over 1 000 iterations. Test predictions were resampled with replacement to recalculate accuracy and weighted F1 scores in this process. Kernel density estimation was then applied to evaluate uncertainty and performance variability. For predictive uncertainty, Shannon entropy was calculated from the class probability outputs of the random forest for each test observation. Samples with higher entropy values corresponded to greater uncertainty in the predicted class. The distribution of entropy values was analyzed across

prediction accuracy (correct vs. incorrect) and further assessed within each stress category. Also, time series analyses were conducted to illustrate temporal dynamics in prediction confidence.

To determine feature importance and interpret the model's predictions, SHapley Additive exPlanations (SHAP, Lundberg and Lee, 2017) was used with the TreeExplainer method. This is a game-theory based approach that attributes the output prediction
275 of a model to its input features, providing an interpretable solution of feature importance that is both local (according to stress type) and global (in overall model for all stress conditions). SHAP values were calculated for all samples in the test set and then combined to create class-specific feature importance rankings. The top 15 VOC features with the highest mean absolute SHAP values were identified for each stress condition. Pairwise comparisons were performed to evaluate feature redundancy and specificity across classes, and the overlaps and unique features were examined. Finally, potential stress-related chemical
280 fingerprints were identified after using the SHAP values and their influence on the predictions for that specific stress.

2.2.2 Positive matrix factorization

To cross-investigate the random forest outcomes, we performed PMF analysis on VOC species measured by the Vocus-PTR-ToF-MS. The PMF model was used to identify the VOC time series into factor profiles, factor time series, and residuals, thereby isolating characteristic stress-related emission patterns. The PMF model has been widely applied to identify different
285 sources and chemical processes of VOCs measured by PTR-ToF-MS across anthropogenic to biogenic emissions (Bhattu et al., 2024; Gkatzelis et al., 2021; Song et al., 2024). The analysis was conducted separately for beech and oak using the Multi-linear Engine (ME-2) and implemented via the Source Finder (SoFi) package (version 8.6.4.4) with Igor-Pro software (version 9.05). The bilinear PMF model resolved the sample matrix into two non-negative matrices: factor profiles (F) representing characteristic mass spectra and factor contributions (G) representing the temporal evolution of each profile, with an associated
290 residual matrix (E).

The cleaned dataset was used as the data matrix, and error matrices were created by 15 % of the measured concentration, combined with twice the standard deviation observed during periods when the signal remained stable. Before selecting the final factor solution, we went through multiple checks: we checked whether the factor's time series appeared random or lacked a clear pattern, inspected the y axis to determine if the factor's contribution was small or noisy, and checked correlation of the
295 factor's time series with main compounds. We also checked the explained variation to identify which compounds were most strongly linked to each factor. Finally, we looked at the time series of those compounds to assess whether they appeared random or noisy.

Results from PMF (top 15 compounds) and ML-based SHAP (top 15 compounds) analyses were integrated as cross-investigation for comprehensive fingerprint identification. Taken together, the integration of PMF and SHAP results extends
300 the understanding of VOC emission tracers under stresses shown in section 3.6.

3. Results and discussion

3.1 Plants' stress-induced diel emission dynamics

Under pre-stress conditions, terpenoid emissions, specifically monoterpenes (MTs) and sesquiterpenes (SQTs), showed the expected diel cycle, with emissions peaking during the light period and falling at night, consistent with their strong dependence on light. This pattern aligns with established findings that emission rates are modulated by environmental variables such as temperature and light (Furnell et al., 2025). However, exposure to abiotic stressors, particularly heat and the combination of ozone and heat, results in the loss of their distinct diel behavior. MT ($C_{10}H_{16}$, m/z 137.13) emissions lose their clear diel behavior under severe heat stress, and so do SQT ($C_{15}H_{24}$, m/z 205.19) emissions from oaks, but not from beeches. Green leaf volatile (GLV) ($C_6H_{10}O$, m/z 99.08) emissions also showed a diel pattern, but emissions increased after nightfall under pre-stress and ozone stress, and are continuously elevated under heat and combined O_3 + heat stress. This nighttime GLV emission is in line with other studies, for instance, Brilli et al. (2011) showed that both poplar and oak showed noticeable bursts of GLV emissions following transitions from light to dark, even without stress or wounding. The authors attributed these transient increases to physiological changes in membrane stability and pH associated with darkening.
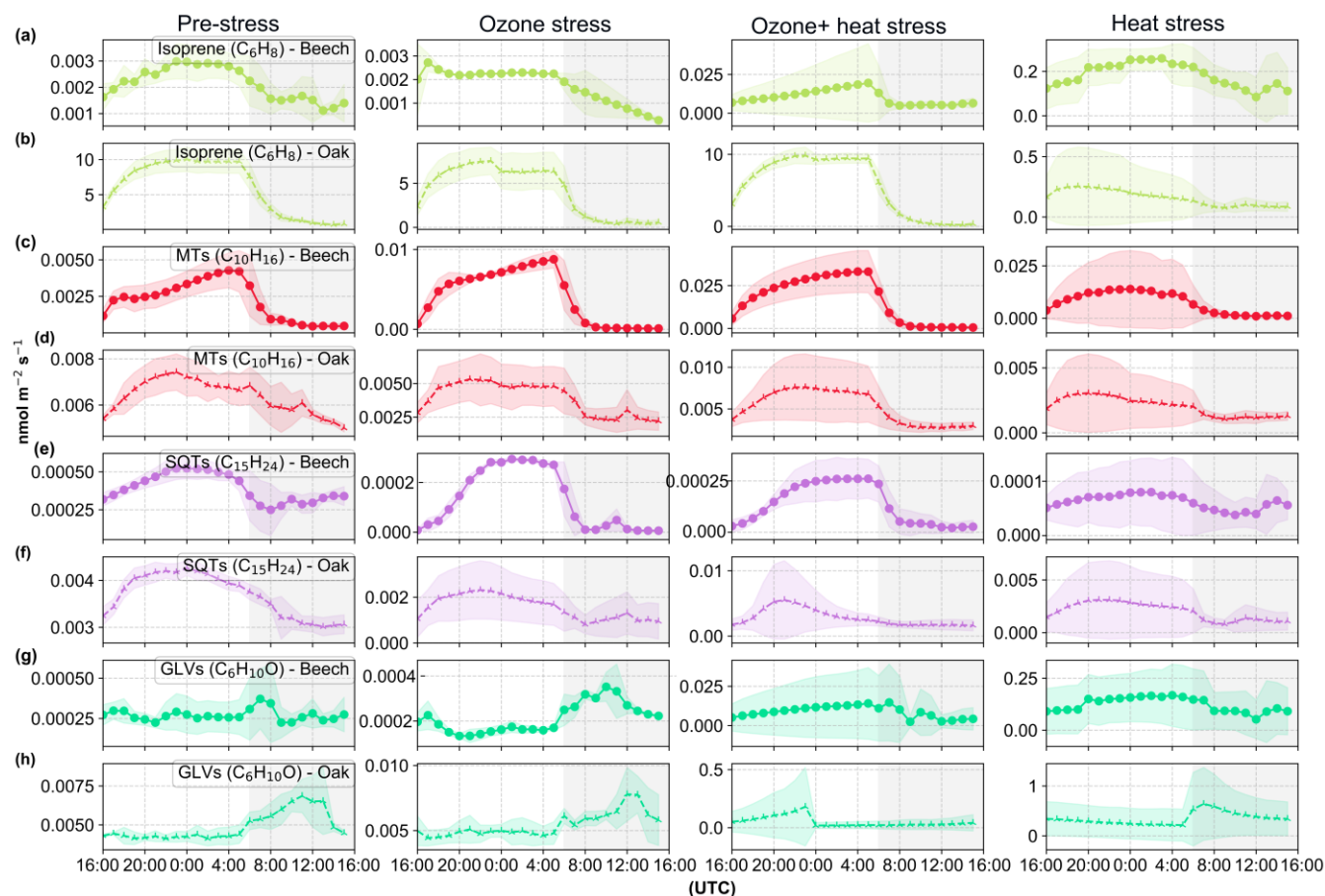
Figure 2. Diel variation in isoprene, monoterpene (MTs), sesquiterpene (SQTs), and green leaf volatile (GLVs) emissions from beech (a,c,e,g) and oak (b,d,f,h) under four conditions: pre-stress, O₃ stress, heat stress and O₃ + heat. On the x-axis, the unshaded region (16:00–6:00 UTC) corresponds to the plants' daytime (lights on), while the grey shaded region represents the plants' nighttime (lights off). Data points are diel averages and shaded areas around them represent the standard deviation.

3.2 Species and stress matter: Beech vs Oak behave differently beyond additive reaction to combined stressors

Isoprene ($C_5H_9^+$, m/z 69.069) emissions were influenced by various stress conditions, with the highest emissions observed under heat stress for both species (Fig. 3). Under pre-stress (acclimation) conditions, the emission rate for beech was 0.003 (±0.0006, standard deviation) nmol m⁻² s⁻¹, i.e. close to zero, as expected (Karl et al., 2009; Moukhtar et al., 2005). Under heat stress, beech switched from a low/non-isoprene emitter to an isoprene emitter, rising to 0.22 (±0.08) nmol m⁻² s⁻¹ (Fig. 3a). This could be a strategy to increase thermotolerance (Sharkey et al., 2001), as beeches are more sensitive to heat stress than oaks (Raftoyannis and Radoglou, 2002). Ozone stress, on the other hand, led to a reduction in isoprene emissions in beech, consistent with Feng et al. (2019), who reported an 8% decrease in isoprene flux under elevated ozone levels. Under combined stress, isoprene emissions increased moderately (to 0.01 nmol m⁻² s⁻¹) for beech, while oaks showed significantly lower emissions under this condition. Despite the reduction caused by heat and ozone stress, oaks still emitted more isoprene than beeches overall (Fig. 3b). Under combined stress, isoprene decreased significantly. This trend is also observed in Arctic regions (Rinnan et al., 2020) and temperate forests (Van Meeningen et al., 2016, 2017).

The terpenoid emissions varied substantially depending on the stress, and species. Since PTR-MS cannot distinguish between different mono- and sesquiterpene isomers, we here discuss the sum of all $C_{10}H_{16}$ compounds as monoterpenes (MTs) and the sum of $C_{15}H_{24}$ compounds as sesquiterpenes (SQTs), while changes in composition of MT and SQT emissions are discussed below. Monoterpene emissions in beech increased substantially under O₃+heat stress (↑728%) (Fig.3). Beech sesquiterpene emissions decreased across all stress conditions (↓84% under heat), because we induced elevated sesquiterpene emissions pre-stress through cutting a branch. Therefore, this result cannot be generalized. However, a temperature-dependent increase is expected, as shown and parameterized for beech by Moukhtar et al. (2005). Monoterpene emissions from oak were substantially increased by heat stress (88%) and slightly reduced by ozone (24%) and combined stress (17%). Pinto et al. (2010) warned that emissions could be underestimated due to the rapid reactions between ozone and MTs, which may mask the true extent of chemical defenses. This issue was alleviated here by applying ozone stress exclusively during plants' nighttime, flushing out residual ozone in the morning, and reporting the daytime emissions that followed the nighttime stress. Oaks' SQTs emissions substantially increased (0.022 nmol, 430% compared to acclimation) under heat stress. Ozone and combined stress inhibited SQT emissions by ~50% compared to pre-stress conditions in both species. While oxidative stress can sometimes induce SQT emissions, some studies (Vo and Faiola, 2023) have reported a decrease in emissions with ozone exposure. For protection against ozone stress, not the amount but the ozone reactivity of the emissions is decisive (Section 3.3). It is important to note that stress response is usually non-linear and depends on factors such as dose levels. A study on a Central European spruce forest (Bourtsoukidis et al., 2012) found that temperature is a key driver of sesquiterpene emissions

in moderately polluted environments, but when ozone levels surpass a critical threshold, emissions are more closely linked to ozone concentrations.
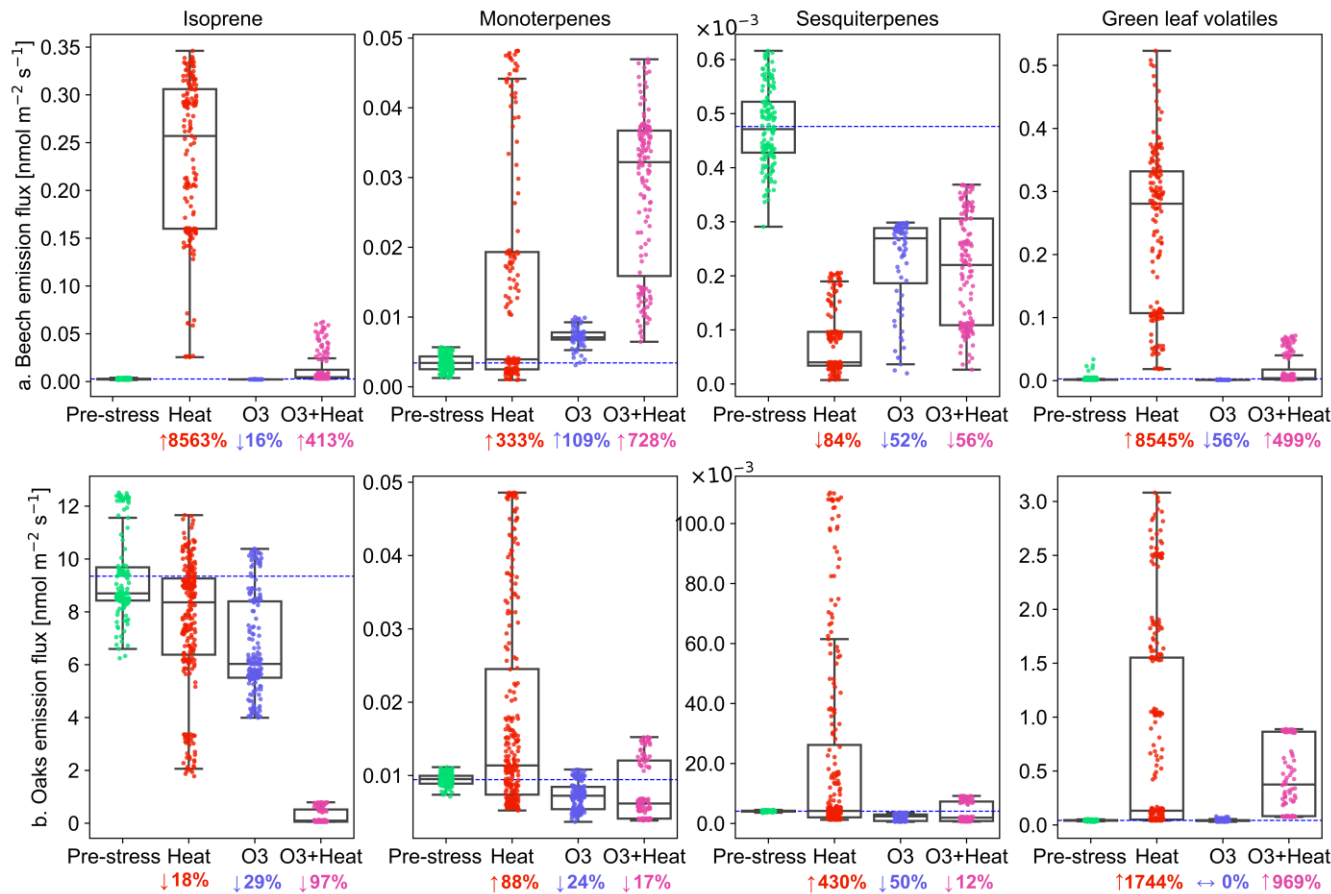
Figure 3. Emissions of isoprene, monoterpene, sesquiterpene, and green leaf volatile emissions from (a) beech and (b) oak under pre-stress, heat, O₃, and combine stress (O₃ + heat) conditions. Boxes represent interquartile ranges, horizontal lines indicate medians, and whiskers show the data spread. The dashed horizontal blue line represents the average pre-stress emission level for reference. Percent changes compared to average pre-stress levels are indicated by ↑ = increase, ↓ = decrease, ↔ = no change.

Green leaf volatiles (GLVs) were substantially increased by heat stress and less by combined stress in both species, while ozone stress barely affected the green leaf volatiles. This aligns with previous studies, which have demonstrated that GLVs are rapidly emitted in response to increased metabolic activity under high temperatures (Cofer et al., 2018; Jardine et al., 2015; Rieksta et al., 2023).

350

355

360 **Table 1 Percentage change in emission fluxes of volatile organic compounds under four biosynthetic pathways, MEP (Methylerythritol Phosphate), LOX (Lipoxygenase), SKP (Shikimate), and MVA (Mevalonate) in beech and oak for three stress conditions. Arrows (▲/▼) indicate increases or decreases in emission relative to the pre-stress baseline (set at 0%). Superscript letters (a–d) denote statistically significant differences within each row, with different letters indicating significant variation among stress events (p < 0.05).**

	Beech				**Oak**			
	Pre-Stress	Ozone Stress	Combined Stress	Heat Stress	Pre-Stress	Ozone Stress	Heat Stress	Combined Stress
MEP	0% [a]	▲55% [b]	▲601% [c]	▲4049% [d]	0% [a]	▼28% [b]	▼18% [b]	▼97% [c]
LOX	0% [a]	▼37% [a]	▲1565% [b]	▲25437% [c]	0% [a]	▼3% [a]	▲4839% [b]	▲2639% [b]
SKP	0% [a]	▲1% [a]	▲30% [c]	▲812% [b]	0% [a]	▼36% [b]	▲373% [c]	▲254% [d]
MVA	0% [a]	▼78% [b]	▲104% [c]	▲4171% [d]	0% [a]	▼57% [b]	▲98% [c]	▲73% [d]

365

Compounds tentatively identified from PTR-ToF-MS measurements were assigned to pathways based on their known biosynthetic origins or related to pathways adapted from Fitzky et al. (2023) (Table S2). These were used to estimate shifts in major plant biosynthetic pathways (LOX, MEP, MVA, and SKP) under different stress conditions. The single and combined stress treatments showed the fundamental differences in how each species reacts to abiotic stress. During heat and combined

370 stress, compounds related to MEP and SKP pathways (Fitzky et al., 2023) were increased, e.g., isoprene, monoterpenes, benzaldehyde ($C_7H_7O^+$, m/z 107.05) and phenethyl acetate ($C_{10}H_{13}O_2^+$, m/z 165.091) (Table S2). Based on these observations, beech activated the plastid-localized metabolic pathways, particularly the MEP and SKP pathways, under both heat and combined ozone-heat stress (Table 1). Stress induced high isoprene and monoterpene emissions (Fig. 3a) under heat and combine stress, possibly by increased enzyme synthesis or accumulation of dimethylallyl diphosphate and geranyl diphosphate

375 (Nogués et al., 2006), indicating a chloroplast-centric metabolic shifting to an active investment in photoprotection (Peñuelas and Munné-Bosch, 2005), redox homeostasis (Loreto et al., 2004), and antioxidant defense (Singsaas, 2000). Notably, while beech also showed substantial increases in emissions from cytosolic pathways (MVA and LOX), including acetaldehyde ($C_2H_5O^+$, m/z 45.03), hexanal ($C_6H_{13}O^+$, m/z 101.09), $C_6H_{11}O^+$ (hexenal, m/z 99.08), hexanol fragment ($C_6H_{13}^+$, m/z 85.10)) these appeared to be part of a broader, integrated metabolic adjustment, coordinated with plastidial pathways (MEP and SKP),

380 following a diel cycle (Figs. 2a,c) contributing a balanced physiological response rather than a primary damage response.
Oak showed a different physiological strategy. Sesquiterpenes, hexenyl acetate ($C_8H_{15}O_2^+$, m/z 143.10), acetaldehyde, hexanal and other compounds (Table-A2) related to LOX and MVA pathways increased significantly during heat stress and under combined stress (except SQTs). The overall LOX and MVA pathway shift during those stressors is significant (Table 1). This points to a more cytosol- and membrane-centric defense mechanism (LOX, MVA) by a dominant activation of the LOX

385 pathway particularly under heat and combined stress. Sesquiterpenes are the primary products of MVA, which significantly increased by heat (Fig. 3b) and are associated with membrane lipid peroxidation (Lõpez et al., 2011) and rapid oxidative signaling (Basile et al., 2025).
The VOC response to ozone alone was relatively low compared to heat or combined stress in both species, likely due to limited stomatal uptake during nighttime exposure, resulting in a weaker trigger of VOC biosynthesis (Table 1), unless combined with

390   additional stressors (e.g., heat). Peron et al.(2021), observed in oak that the combination of ozone with drought altered VOC emission profiles and led to opposing feedback compared to ozone alone. While ozone-induced oxidative stress can stimulate VOC emissions, the magnitude and composition of these emissions are highly dependent on factors such as plant species, developmental stage, stress severity and environmental conditions (Pinto et al., 2010; Renaut et al., 2009), emphasizing the complexity of plant responses to ozone. Mechanistically, ozone exposure leads to intracellular Reactive Oxygen Species (ROS)

395   accumulation and the activation of stress signaling compounds (e.g. jasmonic acid) (Kangasjärvi et al., 2005). Furthermore, chronic ozone exposure leads to downregulation of photosynthetic enzymes such as RuBisCO (Pelloux et al., 2001), suppression of carbon fixation, and activation of offset metabolic pathways including phosphoenol pyruvate carboxylase (Gaucher et al., 2006) and the pentose phosphate pathway (Dizengremel et al., 2008). This metabolic shifting may further constrain VOC production under ozone.

400   We note that the order of events might have influenced how the plants reacted, but there were indications that the order did not overall determine the emissions since, in both beech and oak, the heat stress elicited the largest emissions (Figs. 3 and 5) despite applying combined stress before and after heat stress in oak and beech, respectively.

3.3 Stress reshapes potential atmospheric impacts of BVOC emissions

BVOC emission composition from beech and oaks varied between the stress events (Fig. 4), and so does the reactivity of the

405   sum of the ~80 observed BVOC species with hydroxyl radicals (Fig. 5). Total molar BVOC emissions decreased under O_3 stress in both species compared to pre-stress, were highest under heat stress, and went back to a similar range as pre-stress under combined O_3 + heat stress (Fig. 5a).

Emitted OH reactivity was calculated following

$$OHR_F = \sum_i^n k_{OH,VOC_i} * F_{VOC_i} \qquad \text{(eq. 1)},$$

410   where OHR_F is the emitted OH reactivity in ms^{-2}, $k_{OH,VOC}$ is the reaction rate constant of a VOC with the OH radical in m^3 molecules^{-1} s^{-1}, and F_{VOC} is the flux of the VOC in molecules m^{-2} s^{-1}.

Emitted OH reactivity followed the same pattern as summed VOC emissions, with the highest emitted OH reactivity under heat stress for both species. Summed calculated OH reactivity was higher in oak than beech emissions due to its higher BVOC emissions, especially of highly reactive isoprene.

415
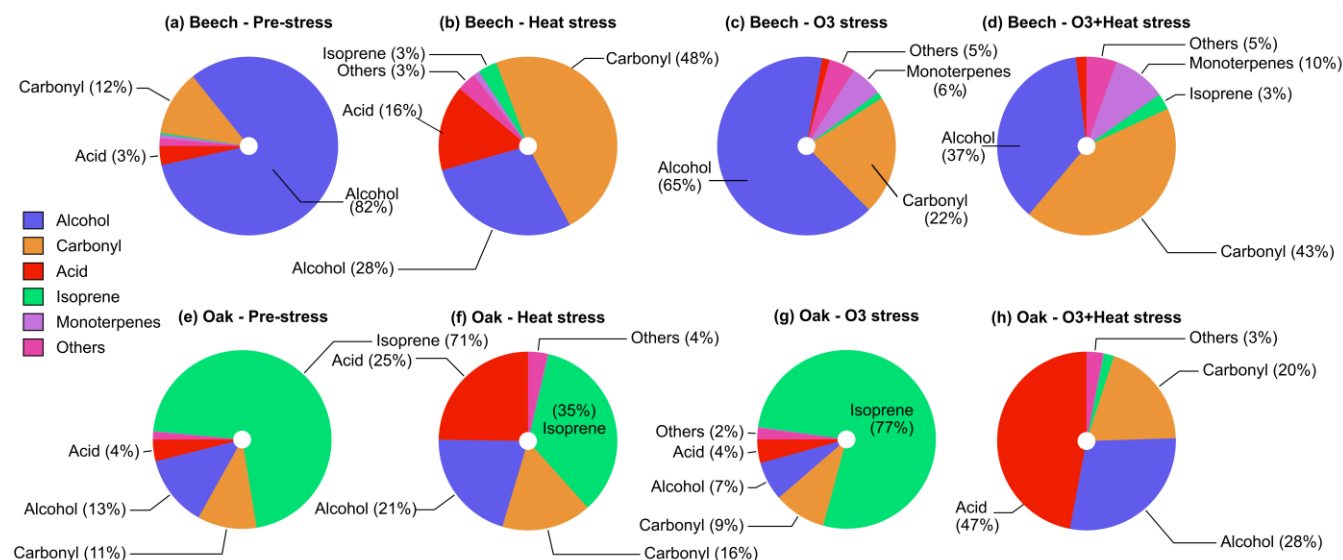
Figure 4. Composition of volatile organic compound classes emitted by (a-d) beech and (e-h) oak under different environmental stress conditions.

Heat stress and combined O_3+heat stress in beech induced emissions with a more diverse emission profile compared to O_3 and pre-stress stress. The emission profile was dominated by alcohols and carbonyls, which together accounted for over 70% of

420 the total emissions and monoterpenes (10%). Among the alcohols, methanol (CH_5O^+, m/z 33.03), and ethanol ($C_2H_7O^+$, m/z 47.05) were the primary contributors, while acetaldehyde, and butanal/methyl ethyl ketone (MEK, $C_4H_9O^+$, m/z 73.06) were the main carbonyls. Monoterpenes (10%) increased substantially under combined stress in beech. Oak emissions were consistently dominated by isoprene pre-stress (71%), as well as under O_3 (77%), while contributions from alcohols, carbonyls and acids increased substantially under heat and combined stress. In oak, acetic ($C_2H_5O_2^+$, m/z 61.02) and propanoic acids

425 ($C_3H_7O_2^+$, m/z 75.04) were the main contributor species of the acid fraction. Carbonyl and alcohol composition similar to that of beech. Both species diversified their emitted BVOC mixture under heat and combined stress compared to pre-stress conditions.

OH reactivity was much higher under heat stress rather than combined ozone and heat stress in both species with different magnitudes. Isoprene dominated OH reactivity emitted from oaks under pre-stress and O_3 stress but not heat and combined

430 stress. In beech, heat stress led to OH reactivity dominated by carbonyls (~25%, mainly acetaldehyde), acids (~27%, primarily acetic acid), and alcohols (~20%, mostly methanol), with isoprene (~12%). When ozone was added on top of heat as a co-stressor, the profile was altered, carbonyls increased to ~30% (now including more acetone), alcohols remained stable (~20%), and with more monoterpenes (~20%) contributions. However, oak showed a different pattern: under heat stress, OH reactivity was driven mainly by isoprene (~56%) and acids (~23%, acetic acid). With combined additive (ozone-heat) stress, there was

435 a shift towards the acid group ~66% and carbonyls to ~14% (notably hexenal and acetaldehyde), while isoprene dropped to just ~4%.

In beech, MTs contributed only 1.7% to emitted OH reactivity under heat stress but ~21% under combined ozone-heat stress. Oak maintained a minimal MTs-OH reactivity contribution (~1%) under both heat and combined stress. Monoterpene composition influenced the monoterpene impacts on OH reactivity (Fig. S3). For example, under heat stress, the MT

440 composition in oak emissions changed from the highest contributor being α-pinene (cyclic) towards a higher contribution of more highly reactive citral (acyclic). In beech, sabinene dominated the monoterpene emissions and reactivity during all parts of the experiment, except during heat stress, when the monoterpene composition diversified and emissions of other highly reactive monoterpenes like phellandrene, citral and limonene increased (Fig. S3). The shift towards more acyclic terpenes under stress is in line with other studies (Graham et al., 2024; Khalaj et al., 2021).

445 O_3 stress substantially reduced total BVOC emissions in both beech (~700%) and oak (~23%) compared to pre-stress levels, resulting in a corresponding drop in total OH reactivity by ~200% in beech and ~7% in oak (Fig.5). Interestingly, in beech, O_3-stress phase OH reactivity became dominated by terpenoids (MTs, SQTs), ~25% of total reactivity, compared to just ~10% during the pre-stress phase. Oak maintained a consistently isoprene dominated OH reactivity profile (~90%) in both stress phases. Physiologically, O_3 alters stomatal regulations and oxidative damage to leaf tissues (more in section 3.2), reducing

450 BVOC biosynthesis and de novo emissions. These emission discrepancies between the species under the same stress also carry the species-dependent stress-action message. While beech appears to shift toward a plastid-centric investment in diverse terpenoid defenses, oak maintains a sustained isoprene production. Moreover, SQT emissions during O_3 stress showed the highest fraction of caryophyllene (Fig. S4), which is among the most reactive sesquiterpenes towards ozone, which could be a potential strategy for protection against oxidative stress.

455 Although our experiments showed species-specific differences in OH reactivity of BVOC emissions under different stress conditions, one consistent pattern appeared: heat stress consistently elevated atmospheric OH reactivity. This potentially reduces the availability of atmospheric oxidants for other trace gases and can slow down the breakdown of key pollutants (e.g., methane, CO). During heatwaves, elevated VOC emissions combined with high OH reactivity can significantly contribute to the formation of tropospheric ozone (depending on NO_x concentration) and secondary organic aerosols. This effect will be

460 more pronounced in urban and semi-urban areas, where biogenic and anthropogenic emissions interact, especially under intense sunlight.
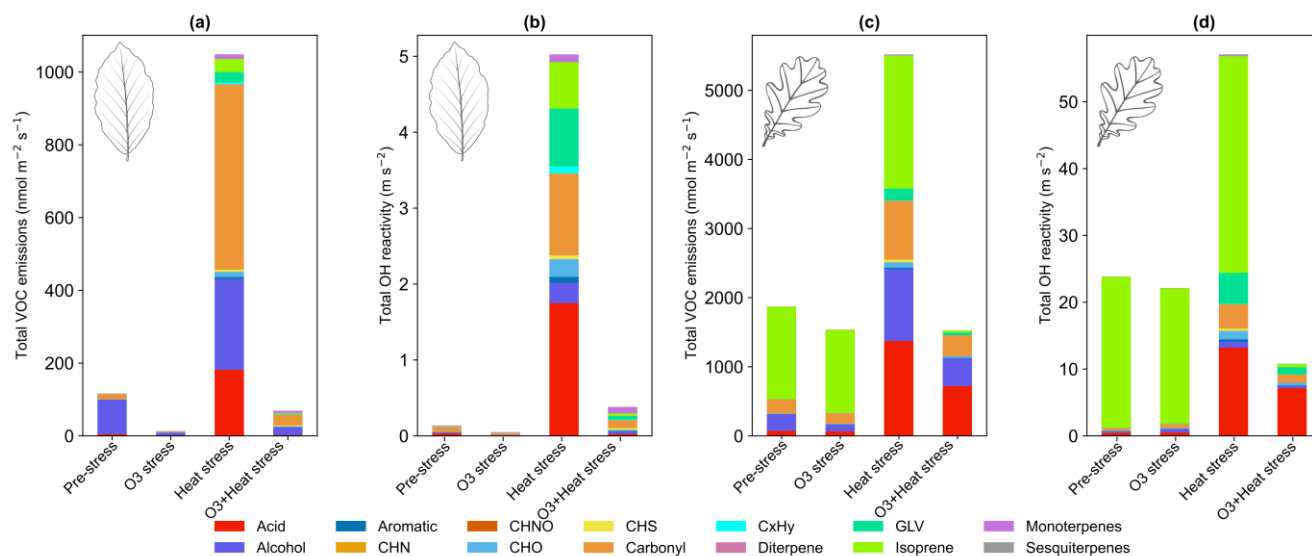
Figure 5 Total volatile organic compound emissions under different stress conditions and their corresponding calculated OH reactivity contributions for (a,b) beech and (c,d) oak .

465 Comparing with field studies, Churkina et al. (2017) showed that biogenic VOCs contributed ~60% to ozone formation during the 2006 Berlin heatwave. Additionally, Zhu et al. (2024) showed that the combination of terpenoids and NOx accounted for more than 55% of the maximum daily 8-hour average ozone formation in Los Angeles. Air quality simulations over Paris during June–July 2022 reported urban tree emissions increased secondary organic matter by an average of 5% (up to 14% during heatwaves) and ozone concentrations by 1% on average (up to 2.4% during heatwaves), with localized increases

470 (Maison et al., 2024). Oak and beech are common tree species found in central and northern European urban and peri-urban areas (Jandl et al., 2025). Our observations, showing that OH reactivity of emissions under heat stress conditions increases by ~97% (beech) or ~58% (oak), support the expectation that ozone pollution in urban areas may increase with more frequent heat waves.

In the real world, especially in an urban atmosphere, several stressors occur at the same time, so that a discussion of additive

475 stress is important. Based on our experiment, beech trees increase their OH reactivity of emissions by ~60% under combined ozone and heat stress, whereas oaks reduce it by ~54%. In the context of European cities and forests, this becomes especially important. Central and Western Europe, including countries like Germany, has large areas dominated by European beech (e.g., in Germany 14.8%), which may lead to increased atmospheric oxidation potential. Naturally, with species heterogeneity in forests, compensatory effects are possible: one species may increase while another decreases OH reactivity, and OH reactivity

480 may be not change substantially overall. A critical concern is the physiological consequences of prolonged additive stress, as evidenced by our experiment, where all plants wilted and died by the end of the combined stress period. Beyond atmospheric consequences, additive stress poses a potential threat to tree vitality and forest ecosystem resilience.

3.4 Random forest model

3.4.1 Consistency and uncertainties

485   The classification matrix for all classes from the trained random forest model for beech and oak shows precision and recall of 0.95 to 1.0 (Figs. 6a-b). Model evaluation was not restricted to standard classification metrics but was extended to explore the classification's consistency, reliability, and uncertainty. Shannon Entropy (uncertainty in prediction) was used to quantify the classification confidence (Figs. 6c–d). Most predictions have low entropy for most samples, and a smaller number of predictions have moderate to high entropy (but less than the threshold). The overlay of correct and incorrect classifications

490   (Figs. 6e–f) also indicated that the most misclassified samples were associated with comparatively high entropy; no entropy values randomly spiked across all conditions. In addition, the time series entropy (see Figs. S5(d) and S6(d)) showed that most classifications were made with high certainty (entropy < 0.6), though slight increases occurred under combined O_3 + heat stress, potentially reflecting overlapping BVOC patterns and the model's sensitivity to complex stress signals. Performance stability was also checked across classes; bootstrapped distributions of classification scores with low variance (Figs. S5(e-f),

495   S6(e-f)) indicate the model's consistency. These evaluations confirmed that trained models are useful in classifying stress types.
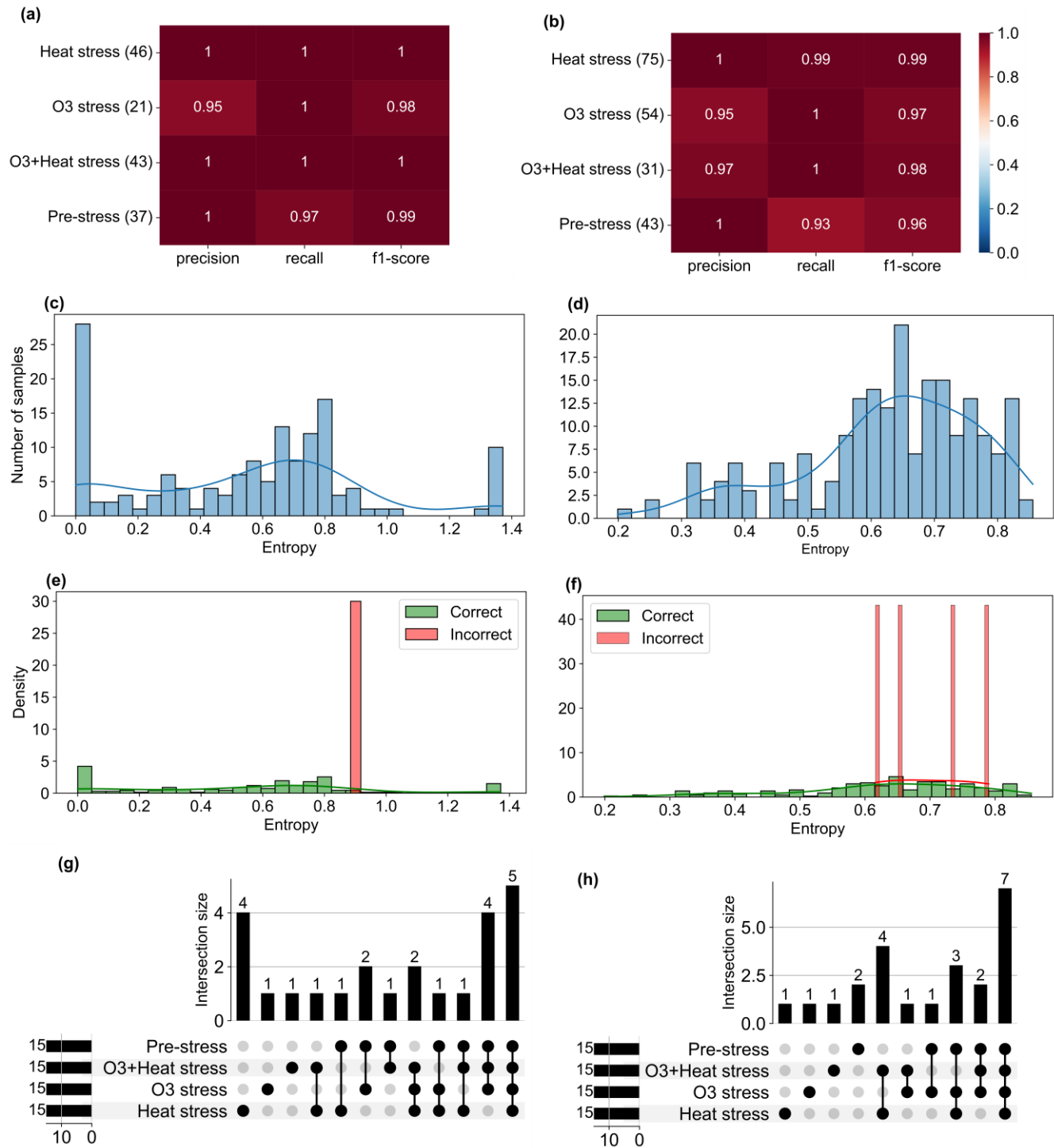
Figure 6. Performance metrics, uncertainty, and misclassification analysis of the Random Forest model for stress classification in (left) beech and (right) oak. (a–b) Precision, recall, and F1-score for each stress class based on the test set. Numbers in parentheses indicate the number of test samples per class. (c–d) Distribution of Shannon entropy values of predicted class probabilities across

all test samples. (e–f) Entropy distributions of correctly and incorrectly classified samples. (g–h) Plots showing intersections of SHAP-identified top 15 stress markers among the four stress classes. Bars represent the number of ions unique to or shared between classes. Insets indicate total counts.

3.4.2 SHAP resolved stress fingerprints

505   SHAP values from Random Forest models (Figs. A1 and A2 in the Appendix A) were used to identify stress-specific compound fingerprints for both beech and oak, as well as interspecific differences associated with stress conditions. Beech primarily depended on a limited number of compounds under each stress scenario (Fig. 7a). In the O_3 stress condition, markers such as propanol ($C_3H_9O^+$, m/z 61.06), methanol (CH_5O^+, m/z 33.03), ionone ($C_{13}H_{21}O^+$, m/z 193.15), and toluadehyde ($C_8H_9O^+$, 121.06) were most prominent, typically contributing with positive SHAP values when suppressed or low emission flux (Figs.

510   7a and A1). These patterns point toward ozone-induced suppression of certain biosynthetic pathways (details section 3.2). Under heat stress, the most dominant contributors included C5 carbonyls ($C_5H_{10}O^+$, m/z 87.08), methyl-vinyl-ketone(MVK, $C_4H_7O^+$, m/z 71.05), phenethyl acetate ($C_{10}H_{13}O_2^+$, m/z 165.01), isoprene, benzoid fragments ($C_6H_7^+$, m/z 79.05, possibly from shikimate pathway products), hexanal ($C_6H_{13}O^+$, m/z 101.09) and cumenol ($C_9H_{12}OH^+$, m/z 137.09). Their increased emissions significantly shifted predictions towards the heat stress class. These BVOCs reflect thermal degradation and markers of heat

515   stress. Interestingly, under combined O_3 + heat stress, monoterpenes ($C_{10}H_{17}^+$, m/z 137.13) were strongly activated (Fig.3a) and have high positive SHAP values (Figs. 7 and A1d), forming a unique and dominant fingerprint for beech under O_3+heat stress.

Similar to beech, under ozone stress, oak showed several BVOCs such as propanol, acetaldehyde, sesquiterpenes and pyruvic acid were identified with high SHAP values, despite their low absolute intensities in ozone-stressed samples. The classifier

520   assigned strong predictive importance to their reduced presence, meaning lower emissions (Table S4) of these features were informative for ozone-related stress discrimination. Such low-emission driven feature patterns highlight that the model's decision was not driven by elevated emissions but rather by reducing specific volatiles during ozone exposure. Oak's heat stress fingerprints were primarily shaped by elevated pyruvic acid ($C_3H_5O_3^+$, m/z 89.02), formic acid ($CH_3O_2^+$, m/z 47.01), toluadehyde, isoprene, and phenol ($C_6H_7O^+$, m/z 95.05) emissions (Fig. 7b). The combined O_3 + heat stress condition showed

525   a compound profile largely driven by markers shared with the individual stress states, but with amplified effect sizes. Particularly, sesquiterpenes, MVK, phenethyl acetate ($C_{10}H_{13}O_2^+$, m/z 165.09), benzoid fragments, formic acid, and ionone were dominant BVOC fingerprints.

The interaction was checked to identify stress-specific and their BVOC overlaps across classes. A limited number of BVOC (Fig. 6g-h) were unique to individual stress conditions among the top 15 BVOC features in both species. Several BVOCs

530   consistently appeared as markers for specific stress types, independent of species, while others showed species-specific stress. These overlapping BVOC fingerprints or signatures imply that certain VOCs may reflect core metabolic responses to abiotic stress, regardless of species-specific physiology.
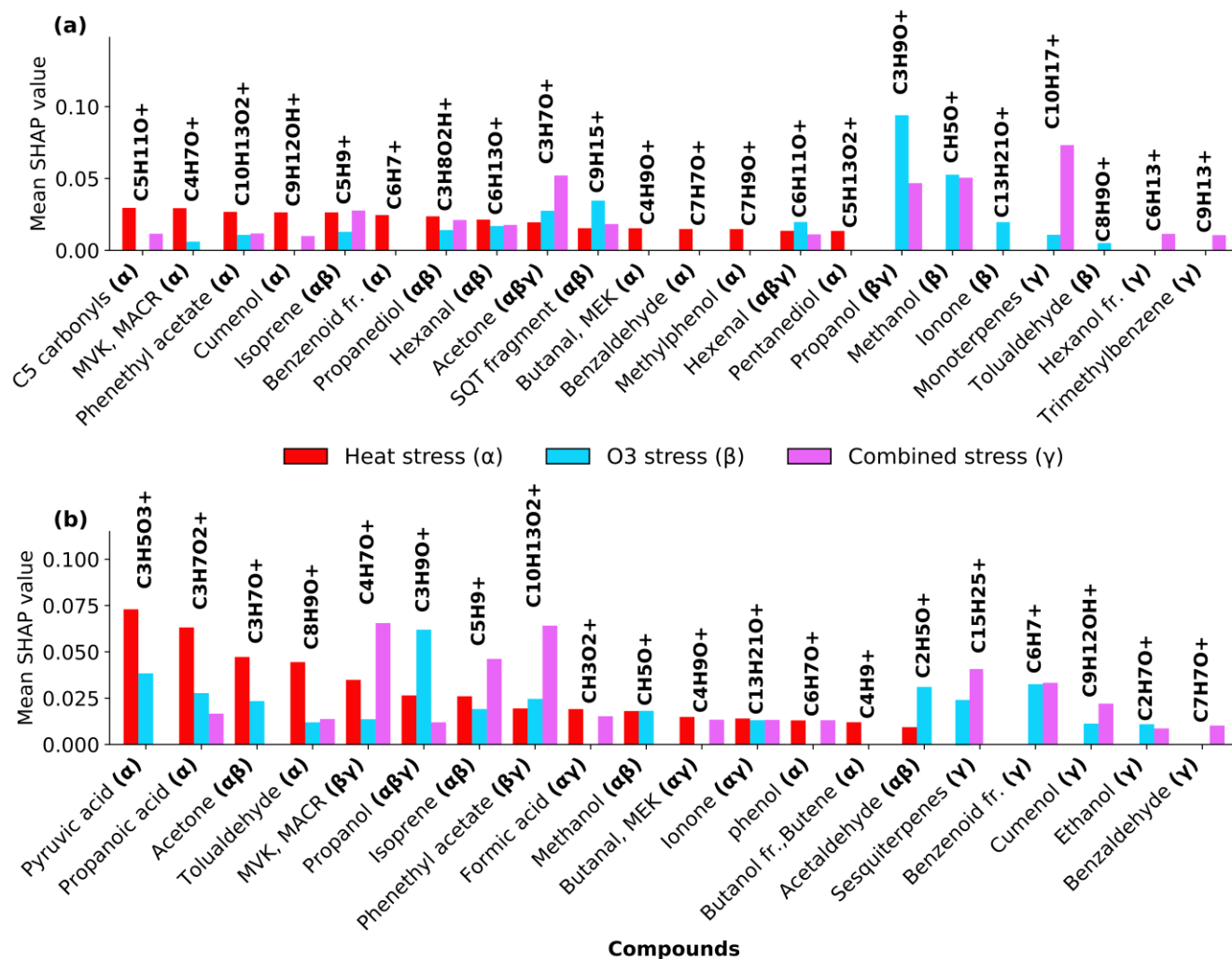
Figure 7 SHAP-based (SHapley Additive exPlanations) feature importance of volatile organic compounds (VOCs) for classifying stress conditions in beech (a) and oak (b). "fr." refers to fragments. Bar plots show the mean SHAP values of potential VOCs fingerprint under heat stress (α), ozone stress (β), and combined O_3 + heat stress (γ).

3.5 Positive matrix factorization

3.5.1 PMF factor interpretation

PMF was used to apportion the stress profile and identified a six-factor solution for both beech (Fig. 8) and oak (Fig. 9). Details about the PMF analysis and the rationale for selecting the six factors are provided in section 2.2.2 and Appendix B.

In Beech, factor-1 is characterised as the "Pre-stress or baseline factor" because it shows consistent and low signal intensity throughout the period (Fig. 8). Additionally, it has weak correlations between the top contributing VOCs and with the factor-time series, and the explained variance for these compounds was minimal. This reflects the background emissions under

unstressed conditions. Factor 2 is termed the "late heat response" factor due to its steady flux increase (after ~38°C) beginning
toward the end of the O₃+heat phase and continuing into the heat stress period. This gradual rise coincides with the sharp
increase in chamber temperature, indicating that this factor likely captures delayed thermal stress responses. Factor 3 is
identified as the "plant decay" factor, as it becomes prominent after the stress, and the time series suggests a delayed emission
peak independent of immediate heat or ozone exposure. This temporal dissociation implies involvement in cell lysis, consistent
with the observation that all plants had wilted by the end of the experiment. Factor 4 is considered the "combined stress" factor,
as it shows a distinct peak coinciding with the period of simultaneous O₃ + heat exposure. The time series shows a rapid, stress-
synchronous response. Factor 5 is designated the "severe heat stress" factor, characterized by a sharp and isolated peak during
the highest temperature phase of the experiment (42 °C), without overlap from ozone exposure. Factor 6 is interpreted as the
"early heat stress" factor, with a narrower temporal window earlier than the main O₃+heat peak and displays an earlier response
to rising temperatures (~36–38 °C) before full stress onset.

In Oak, Factor 1 is identified as the "Pre-stress or baseline factor" due to its moderate contribution across all phases, including
the pre-stress and early ozone exposure, without showing any substantial sharp peak (Fig.9). Its VOC composition is broad
but with low correlation (without considering isoprene, oak generally emits isoprene) and explained variance for most top
compounds, likely representing constitutive emissions and ambient-level biological activity. Factor 2 is associated with the
"O3+heat stress," peaking sharply during the overlapping ozone and heat phase. Factor 3 is labelled the "late heat stress factor,"
as it indicates a delayed increase after the peak heat stress events have abated. Factor 4, termed the "initial heat stress factor,"
dominates during the standalone heat phase and peaks just after the onset of heat stress. Factors 5 and 6 are described as the
"severe heat stress," showing the maximum contribution during the peak heat stress temperature (~42 °C), after which they
consistently decline.
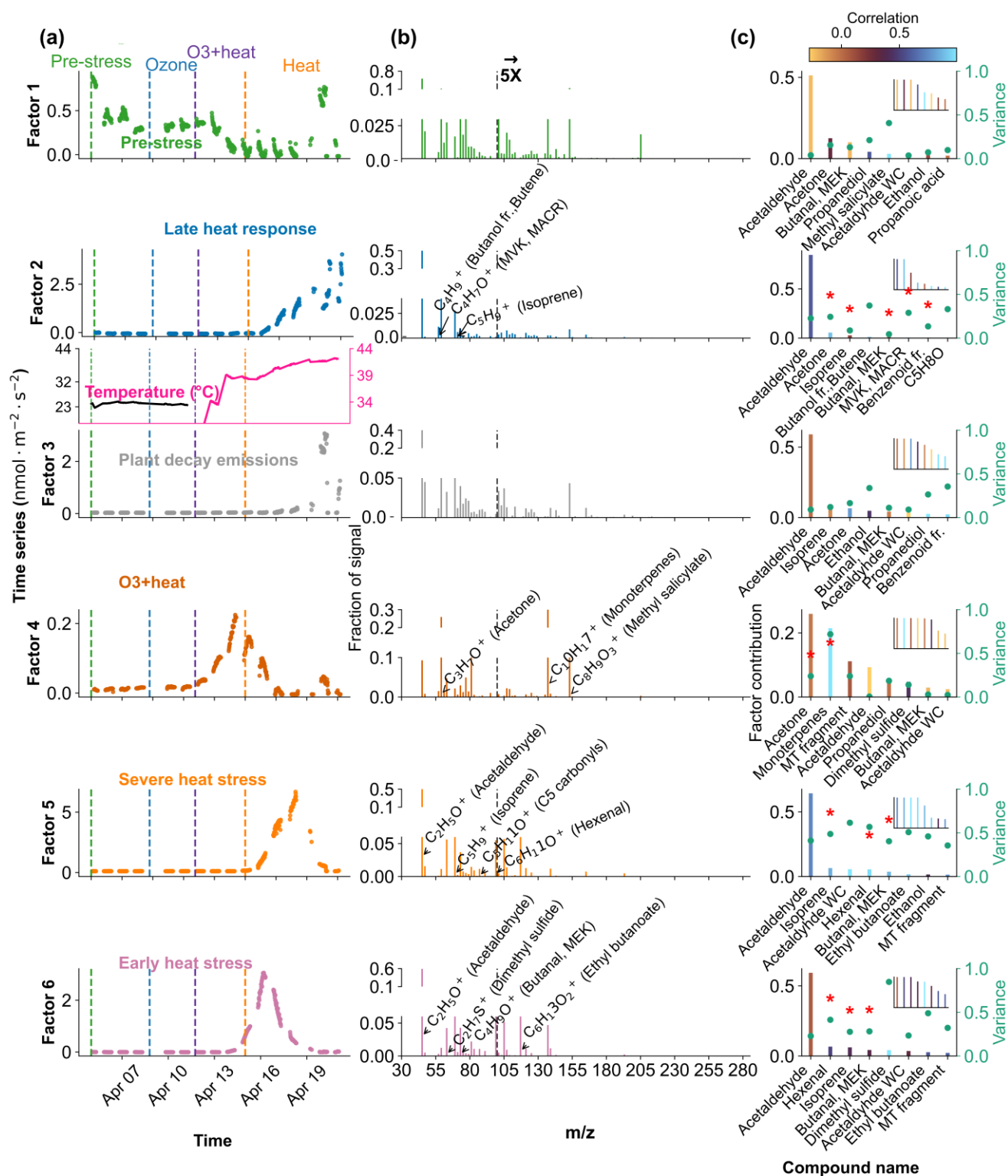
565 **Figure 8. Positive Matrix Factorization (PMF) analysis of VOC emission profiles from beech under different environmental stress conditions. (a) Time series of a six-factor PMF solution. Colored vertical dashed lines indicate the starting of different stress phases. (b) Corresponding mass spectra (m/z profiles) of each factor and their relative signal contributions, m/z 100–280 are scaled by a factor of 5. (c) Top 8 compound markers for each factor. Bar plots show the relative contribution of specific compounds, while green dots represent the correlation coefficient with the respective factor time series. Color shading indicates their correlation with the**
570 **corresponding factor timeseries, and asterisks (*) denote compounds that were also identified as fingerprints by the machine learning.**

3.5.2 PMF-resolved stress-VOCs profiles for stress fingerprints

The early heat stress factor for beech (Fig.8) was characterized by hexenal, isoprene, ethyl butanoate ($C_6H_{13}O_2^+$, m/z 117.09), MEK, and monoterpene fragments ($C_6H_9^+$, m/z 81.07). Similar fingerprint patterns were also seen in the severe heat stress and
575 late heat response factors. Additionally, the severe heat stress factor uniquely showed contributions from MVK, benzenoid fragments, and C_5H_8O ($C_5H_8OH^+$, m/z 85.06), making it apart from the other heat-related factors. These findings are consistent with studies showing that temporary heat stress triggers the biosynthesis of GLVs (e.g, hexenal) and isoprene, which serve as rapid markers of membrane perturbation and ROS signaling within leaf tissues (Bao et al., 2023; Kleist et al., 2012a; Turan et al., 2019). Particularly, isoprene is well-documented to increase cell membrane stability during thermal stress and is frequently
580 emitted by deciduous trees under elevated temperatures (Bao et al., 2023; Iwasa et al., 2024). As heat stress persists, the VOC emission for late heat stress remains similar but becomes more complex with contributions from MVK, benzenoid fragments, and C_5H_8O ($C_5H_8OH^+$, m/z 85.06). MVK emissions are predominantly endogenous under thermal stress (Cappellin et al., 2019), and benzenoid compounds accumulate during acute heat exposure (Liu et al., 2022), representing the activation of distinct stress-related metabolic shifts over time.

585 The O_3 + heat stress factor showed a distinct VOC response and was strongly dominated by monoterpenes ($C_{10}H_{17}^+$, m/z 137) with additional supporting signals from monoterpene fragments, acetone ($C_3H_7O^+$, m/z 59.04), Methyl salicylate ($C_8H_9O_3^+$, m/z 153.05) and propendiol ($C_3H_8O_2H^+$, m/z 77.05). Elevated monoterpene emissions are generally attributed to temperature-induced responses in plants and have even been described as a 'thermometer of plants' (Jardine et al., 2017). Furthermore, monoterpenes serve as antioxidants, helping to mitigate oxidative stress caused by both elevated temperatures and ozone by
590 quenching ROS and contributing to cross-tolerance against double abiotic stresses. On the other hand, acetone emissions have been associated with cellular decay and ozone-induced damage, as described in several studies (Davison et al., 2008; Loubet et al., 2022; Wu et al., 2019).

The plant decay factor was temporally shifted toward the end of the experiment, particularly after the peak of combined O_3 + heat stress. The chemical profile was not distinct from the other factors, with typical stress marker compounds, e.g.,
595 acetaldehyde, ethanol, acetone, hexenal, benzoid fragments, and isoprene. Most of these low m/z compounds, notably ethanol acetone, and acetaldehyde, are by-products of altered respiratory activity and fermentative metabolism under high temperature as discussed before, may be due to cell-lysis.
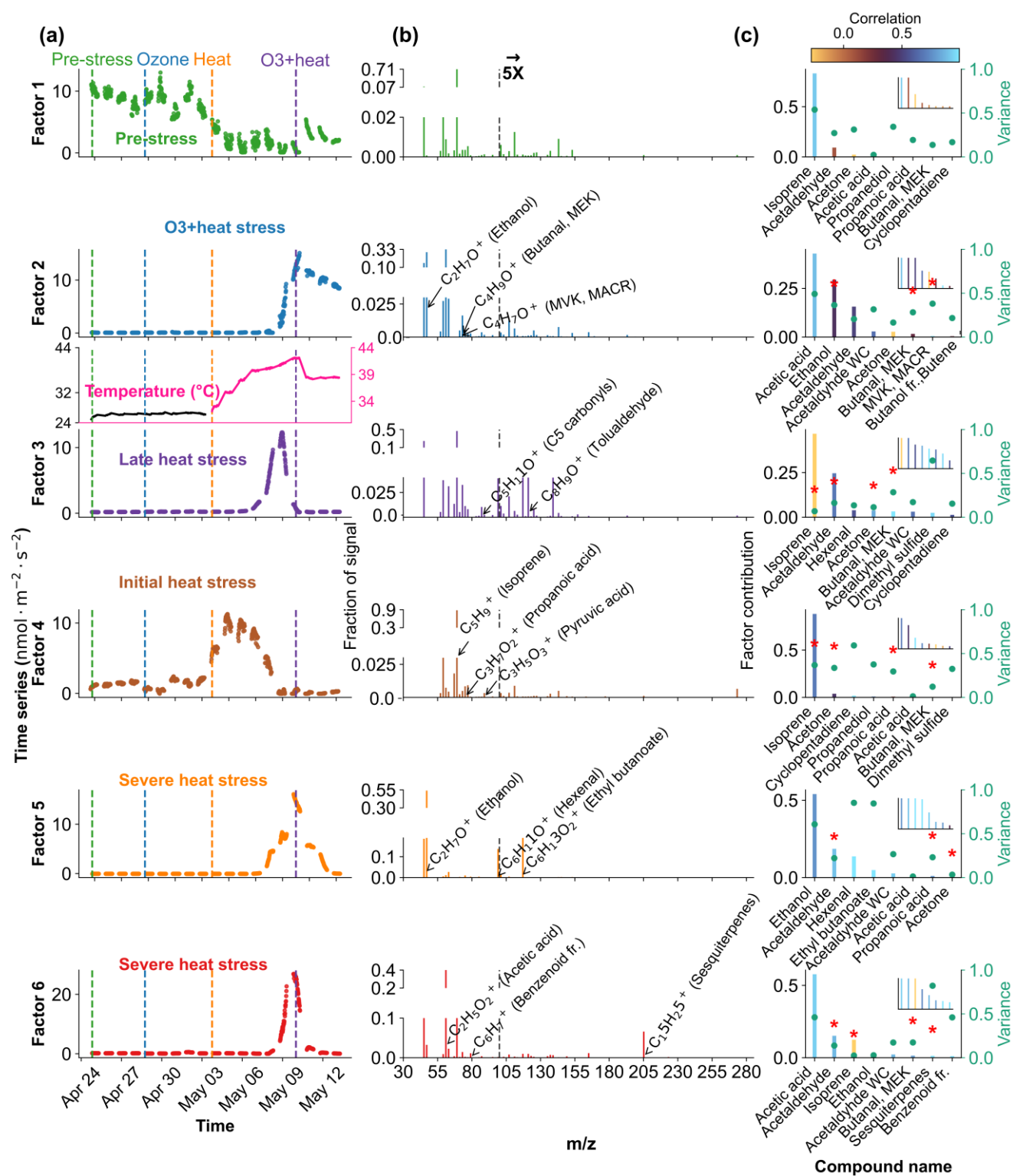
Figure 9. Positive Matrix Factorization (PMF) analysis of VOC profiles in oak under different environmental stress conditions. (a) Time series of a six-factor PMF solution. Colored vertical dashed lines indicate the starting of different stress phases. (b) Corresponding mass spectra (m/z profiles) of each factor and their relative signal contributions, m/z 100–280 are scaled by a factor of 5. (c) Top 8 compound markers for each factor. Bar plots show the relative contribution of specific compounds, while green dots represent the correlation coefficient with the respective factor time series. Color shading indicates their correlation with the corresponding factor timeseries, and asterisks (*) denote compounds that were also identified as fingerprints by the machine learning.

In oak (Fig.9), initial heat stress was characterized by distinct fingerprints of isoprene, propanoic acid, MEK, pyruvic acid ($C_3H_4O_3^+$, m/z 87), and cyclopentadiene. Interestingly, a similar VOC signature reappeared during the late heat stress phase, and this recurrence suggests that both the duration and intensity of thermal exposure led to repeated cycles of oxidative metabolism and membrane adjustment. Elevated isoprene is a hallmark VOC in oaks and responds sharply (Table S4) to rapid temperature increases as thermoprotectant (Li et al., 2010). Also, the co-presence of pyruvic acid, MEK, and propanoic acid could be due to activated glycolytic and pyruvate turnover pathways to supply energy for thermal resilience (Loreto and Schnitzler, 2010). In contrast, severe heat stress induced a distinct chemical signature dominated by sesquiterpenes, benzenoid fragments, hexanal, and ethyl butanoate. These compounds are often linked to more advanced or prolonged heat stress responses as discussed earlier in beech, potentially involving membrane degradation and lipid oxidation.

The factor associated with the combined O_3 + heat stress showed unique dominance of acetone, acetic acid, MVK, MEK, butene, and ethanol. Acetone has been associated with cellular decay and ozone damage in multiple studies (Davison et al., 2008; Loubet et al., 2022; Wu et al., 2019). Notably, the co-emission of MVK and MEK supports the mechanistic model by Cappellin et al. (2019), which showed that MEK could be produced biogenically from MVK within plant tissues via stress-induced pathways decoupled from isoprene biosynthesis. The presence of MVK and MEK in high abundance (Table S4) under combined O_3 + heat stress, but not necessarily under isolated ozone or heat periods, emphasizes that this transformation pathway is particularly prominent when plants simultaneously encounter intensified ozone and heat stress.

3.6 Do ML and PMF tell the same story of stress-specific fingerprints?

Both PMF and ML approaches identified overlapping VOC fingerprints for specific stressors, along with species-specific differences in these fingerprints (Table 2). For example, elevated isoprene appeared as a heat stress marker across both species, signifying it could be a potential universal heat stress marker. Conversely, elevated sesquiterpenes were found as markers only for severe heat stress for oak, which may be related to the non-generalizable sesquiterpene emissions we induced in the beech experiment by having to cut one branch. Stress-BVOCs like acetone, MVK, MEK, and benzenoid fragments, although marked in both species, varied in intensity and timing, showing possible differences in oxidative stress responses or cell membrane degradation (Figs. 8 and 9). Collectively, PMF and ML offer complementary perspectives: PMF elucidates temporal emission patterns, whereas ML identifies the most informative features for distinguishing stress types.

Table 2 Stress-specific volatile organic compound fingerprints in Beech and Oak under heat, ozone, and combined ozone + heat stress. Superscripts (ψ, Φ) denote identification by Machine Learning (ψ) or Positive Matrix Factorization (Φ).

Compound	Stress fingerprint		
	Heat	Ozone	Ozone + heat
Isoprene (C_5H_8)	Beech [ψ+φ], Oak [ψ+φ]		
Monoterpene ($C_{10}H_{16}$)			Beech [ψ+φ]
Sesquiterpenes ($C_{15}H_{24}$)	Oak [ψ+φ]		
MEK (C_4H_8O)	Oak [ψ+φ], Beech [ψ+φ]		Oak [ψ+φ]
MVK (C_4H_6O)	Beech [ψ+φ]		Oak [ψ+φ]
Ionone ($C_{13}H_{20}O$)		Beech [ψ]	
C5 carbonyls ($C_5H_{10}O$)	Beech [ψ+φ]		
Benzoid fragments (C_6H_6)	Beech [ψ+φ],		
Acetone (C_3H_6O)	Beech [ψ+φ], Oak [ψ+φ]		Beech [ψ+φ],
Hexenal ($C_6H_{10}O$)	Beech [ψ+φ]		
Acetaldehyde (C_2H_4O)	Oak [ψ+φ]		
Propanoic acid ($C_3H_6O_2$)	Oak [ψ+φ]		
Ethanol (C_2H_6O)			Oak [ψ+φ]
Methanol (CH_4O)		Beech [ψ]	
Propanol (C_3H_8O)		Beech [ψ]	

3.7 Consequences of a shift to stress-related biogenic VOC emission patterns in a warming climate

Projected climate change trends indicate an increase in the frequency of hot days and heatwaves, leading to compound heat-ozone waves (Hertig et al., 2020; Yang et al., 2022). The relative contributions of various BVOC classes emitted by beech and oak trees are expected to shift significantly due to heat stress (Fig. 7). Thus, urban areas containing such trees may experience a notable alteration in the composition of emitted BVOCs, with biogenic sources becoming increasingly influential on urban air quality. For instance, elevated isoprene and monoterpene emissions during heat stress can enhance ozone formation potential, as these compounds readily react with atmospheric oxidants, thereby raising ozone levels in urban environments where high levels of nitrogen oxides from combustion are present, particularly on hot summer days (Pfannerstill et al., 2024). Moreover, O_3 itself reacts with olefinic BVOCs like isoprene and terpenes to produce additional OH radicals (Di Carlo et al., 2004), creating a positive feedback loop that can amplify BVOC oxidation in the atmosphere. This OH production from O_3-BVOC reactions can further extend tropospheric ozone and secondary organic aerosol formation, compounding the effects of heatwaves on urban pollution levels. Also, the rising prevalence of BVOCs under warmer conditions raises concerns regarding their interactions with anthropogenic emissions. In areas with both high nitrogen oxide levels and high BVOC emissions from vegetation, this loop could drive periodic spikes in ozone and fine particulate matter, contributing to regional pollution events.

4 Conclusion

650 This study provides an investigation of how biogenic volatile organic compounds (BVOCs) are modulated in response to heat and ozone stress, by two dominant deciduous European forest tree species, beech and oak, and to our knowledge, for the first time, in response to the combination of both stressors. Our findings highlight distinct species-specific patterns in the emissions of key BVOCs like isoprene, monoterpenes, sesquiterpenes, and green leaf volatiles, which vary considerably depending on the type of stress encountered. Combined ozone + heat stress elicited emission responses that were distinct from both singular

655 stress applications, highlighting the complexity of real-world stress scenarios where multiple stressors likely happen in combination. In order to facilitate stress identification in future field measurements, we identified stress-specific fingerprint BVOC markers for each stress using machine learning (Random Forest) and cross-validation by Positive matrix factorization (PMF).

Beech switched from a low/non-isoprene emitter to an isoprene emitter under heat stress. While oxidative stress (~ 120 ppb

660 O_3) suppressed the isoprene emissions by 16%, the addition of heat still led to a considerable increase, though less than heat alone. Though Oak is a high isoprene emitter, its isoprene emissions were reduced under stress. Under combined ozone + heat stress, they decreased significantly. Green leaf volatiles were substantially increased by heat stress and less by combined stress in both species, while ozone stress barely affected the green leaf volatiles. Beech activated plastid-localized pathways under heat and combined ozone + heat stress, whereas oak relied on cytosolic and membrane-associated defenses. Total molar BVOC

665 emissions decreased under O_3 stress in both species compared to pre-stress, were highest under heat stress, and went back to a similar range as pre-stress under combined O_3 + heat stress. Emitted OH reactivity followed the same pattern, with the highest emitted OH reactivity under heat stress for both species. Distinct VOC fingerprints were associated with specific stress types in each species. For example, in beech, combined stress was uniquely marked by increased monoterpenes emission. In oak, it was characterized by elevated methyl-vinyl-ketone and ethanol.

670 As a caveat, the experiment involved branch cutting (to fit one beech plant into the plant chamber), which may not fully replicate the acclimation phase of this species properly. The induction of sesquiterpenes through cutting in beech limits the generalizability of some pathway results. Since the duration and intensity of stress influences how much it changes plant emissions, our results may not be generalizable for all ozone, heat, and O_3 + heat situations. Future research could validate our findings through integrative approaches, on the one hand going into biomolecular directions for a better understanding of the

675 plant reactions, and on the other hand photochemical oxidation of the plant emissions to investigate their impact on atmospheric chemistry. The stress-specific BVOC markers identified in this study proposed an auspicious path for rapid stress detection in Beech and Oak, yet their broader applicability across species (in landscape level) or even within different genotypes of the same species remains an open question.

Our findings demonstrate that tree species under combined abiotic stress can either amplify or reduce their contribution to

680 atmospheric reactivity, depending on species-specific physiology and stress magnitude. This has direct consequences for tropospheric ozone formation, secondary organic aerosol formation, and urban air quality, especially during heat waves. As

heatwaves and pollutant stress events become more frequent due to climate change, shifts in VOC emissions and potential dieback in sensitive species like beech could significantly alter atmospheric chemistry, ecosystem function, and carbon budgets. As knowledge on the interactions between multi-stressed trees and the atmosphere grows, these dynamics must be incorporated into regional climate models and policy planning for urban greening and forest management.

Appendix A: SHapley Additive exPlanations: Random Forest
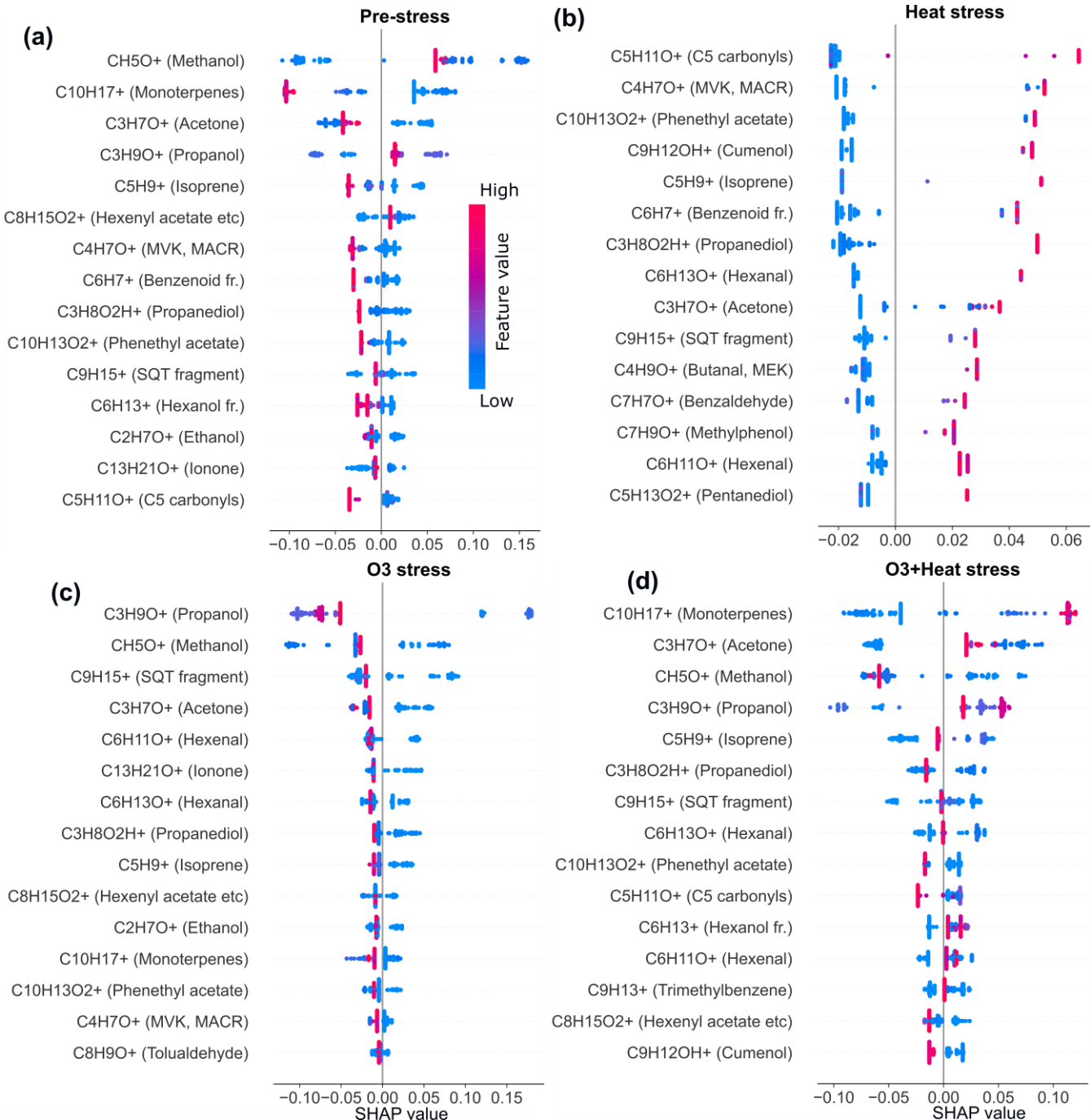
Figure A1. SHAP summary plots based on the trained Beech Random Forest model the top 15 important BVOC features for classifying each stress condition. (a) Pre-stress, (b) heat stress, (c) O₃ stress, and (d) O₃ + heat stress. Each point represents a SHAP value for a specific compound in an individual sample, with colors indicating feature value. Positive SHAP values indicate a stronger association with the predicted stress class.

690
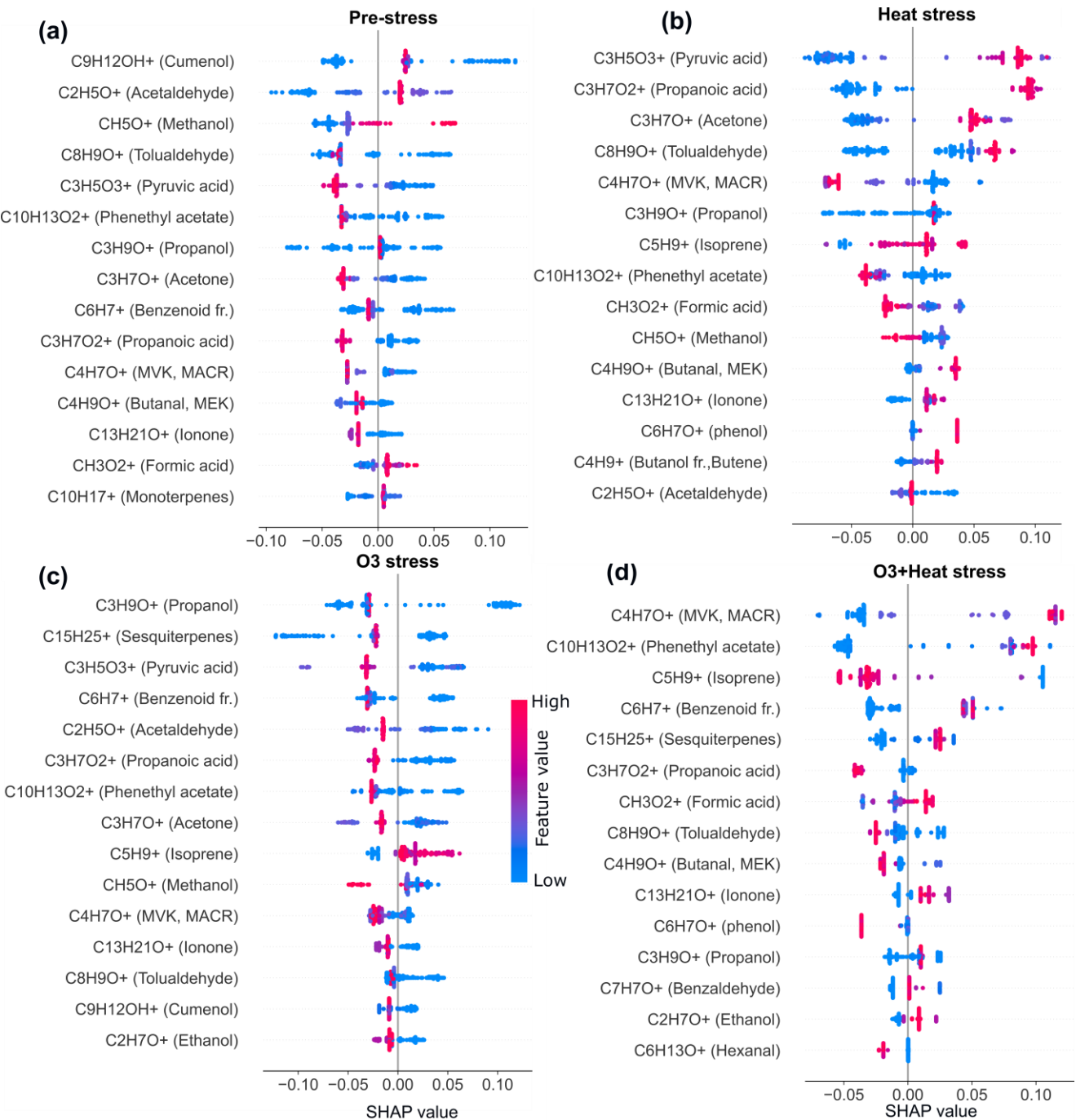
Figure A2. SHAP summary plots based on the trained Oak Random Forest model the top 15 important BVOC features for classifying
695 **each stress condition. (a) Pre-stress, (b) heat stress, (c) O₃ stress, and (d) O₃ + heat stress. Each point represents a SHAP value for a specific compound in an individual sample, with colors indicating feature value. Positive SHAP values indicate a stronger association with the predicted stress class.**

Appendix B: Positive Matrix Factorization (Validation)

In beech and oak PMF, a range of possible solutions 3 to 10 factors were evaluated through a series of quantitative analysis.
700   The choice of the 3 to10 factor range was based on the expected complexity of plant VOC emissions, which are influenced by
multiple overlapping processes including baseline metabolic activity, temperature-induced emissions, ozone responses, or
decay. Solutions with fewer than three factors were excluded from the outset as biologically implausible. Conversely, solutions
above 10 factors tended to produce overly fragmented and unstable profiles, making them less reliable for interpretation and
comparison. As mentioned in section 2.2.2, multiple checks were performed before deciding on the final solution. One last
705   strategy was to test the PMF factor solution, how each factor reproduces the temporal structure of the raw VOC signals, and
the residual (unexplained) signal. All potentially stress-relevant BVOCs (identified through ML) were assessed for
reproducibility and residual (unexplained) signal to ensure the selected factor solution is statistically robust.

For example, for beech, the 3 to 5 factor solutions substantially underestimated monoterpene peaks during combined ozone
and heat stress phases (Fig. B1 (a-c)). On the other hand, solutions with 7 or more factors began to split monoterpenes into
710   separate profiles, introducing artifacts such as unrelated low-level noise contributions (Fig. B1e). Based on this, the 6-factor
solution was selected as it reproduces the peak intensities and temporal patterns without introducing overfitting artefacts or
excessive noise (Fig. B2).

Similarly, for oak, sesquiterpenes were poorly captured in lower-factor solutions (Fig. B3). These high-mass compounds were
either lumped into broad stress-related profiles or ignored altogether, leading to underrepresentation. Only in the 6-factor
715   solution was a distinct and coherent representation of sesquiterpenes observed in Oak, aligning with stress onset and peak
fluxes. Beyond the 6 factors, this signal began to fragment.
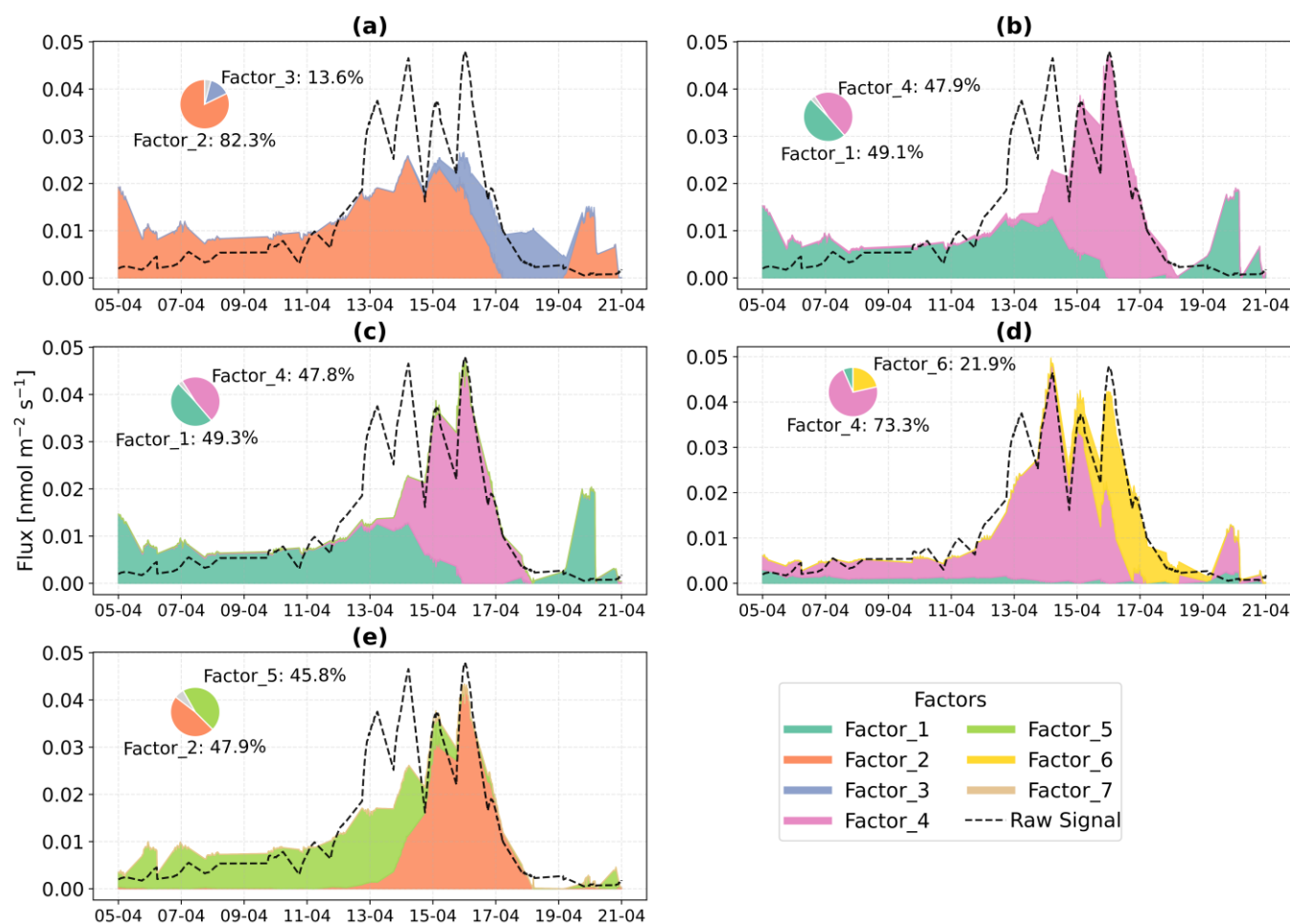
Figure B1. Stacked monoterpene time series showing PMF-resolved factor contributions for 3-factor (a) to 7-factor (e) solutions in Beech. Each subplot represents a different PMF solution. Colored areas correspond to contributions from individual factors, while the white area under the curve indicates unexplained. Inset pie charts represents the total contribution of each factor to the monoterpene signal.
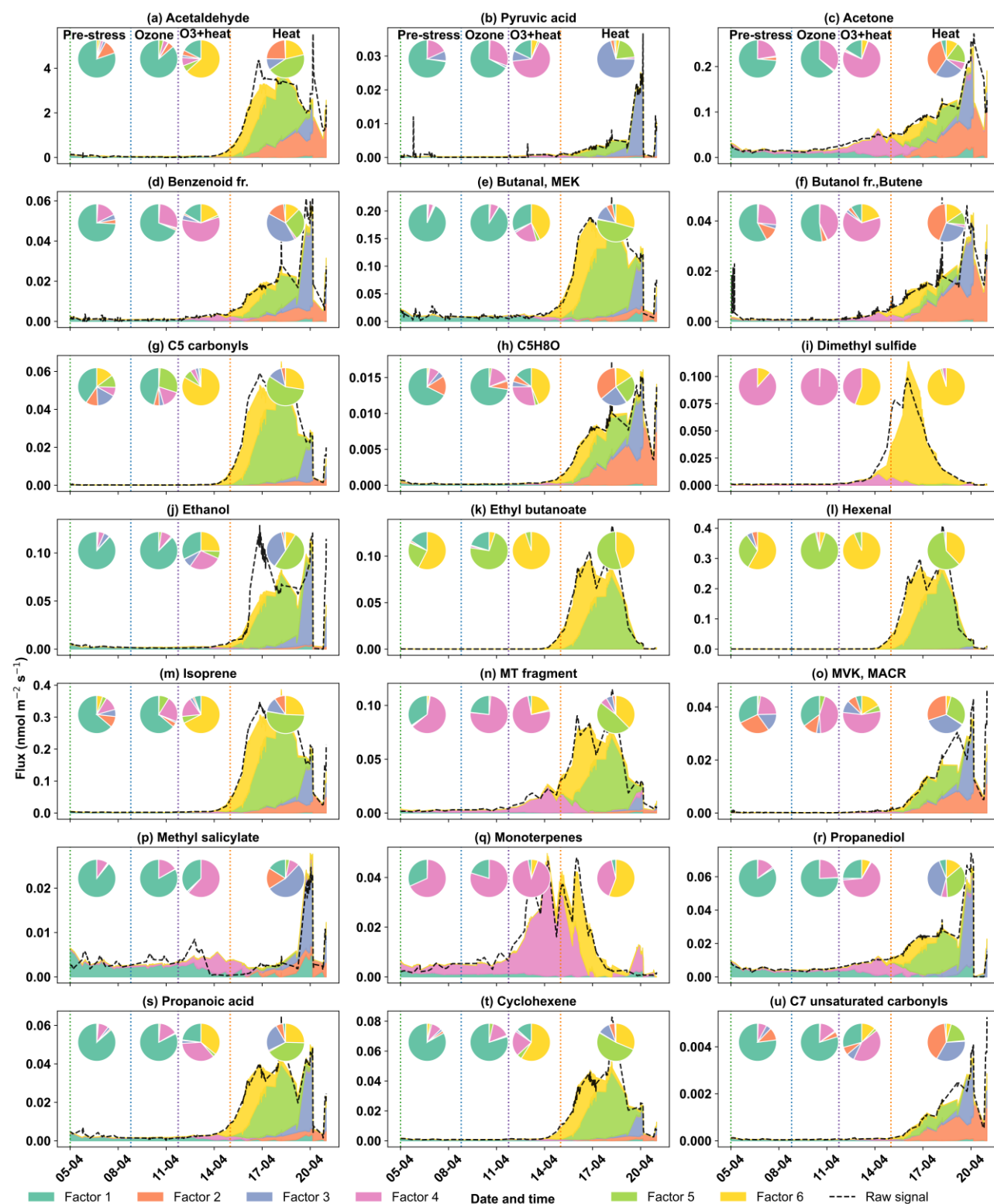
Figure B2 Stacked time series of PMF-resolved contributions for selected BVOC compounds during the Beech experiment. The black dashed lines indicate the original concentration of specific compounds, while stacked colored areas represent contributions from the six PMF-resolved factors. Each compound's emission is displayed across the four stress periods (Pre-stress, O₃ stress, O₃ + Heat stress, Heat stress), separated by vertical dashed lines. Inset pie charts show the relative contribution of each factor to compound emissions within each stress period, as a factor dominance.
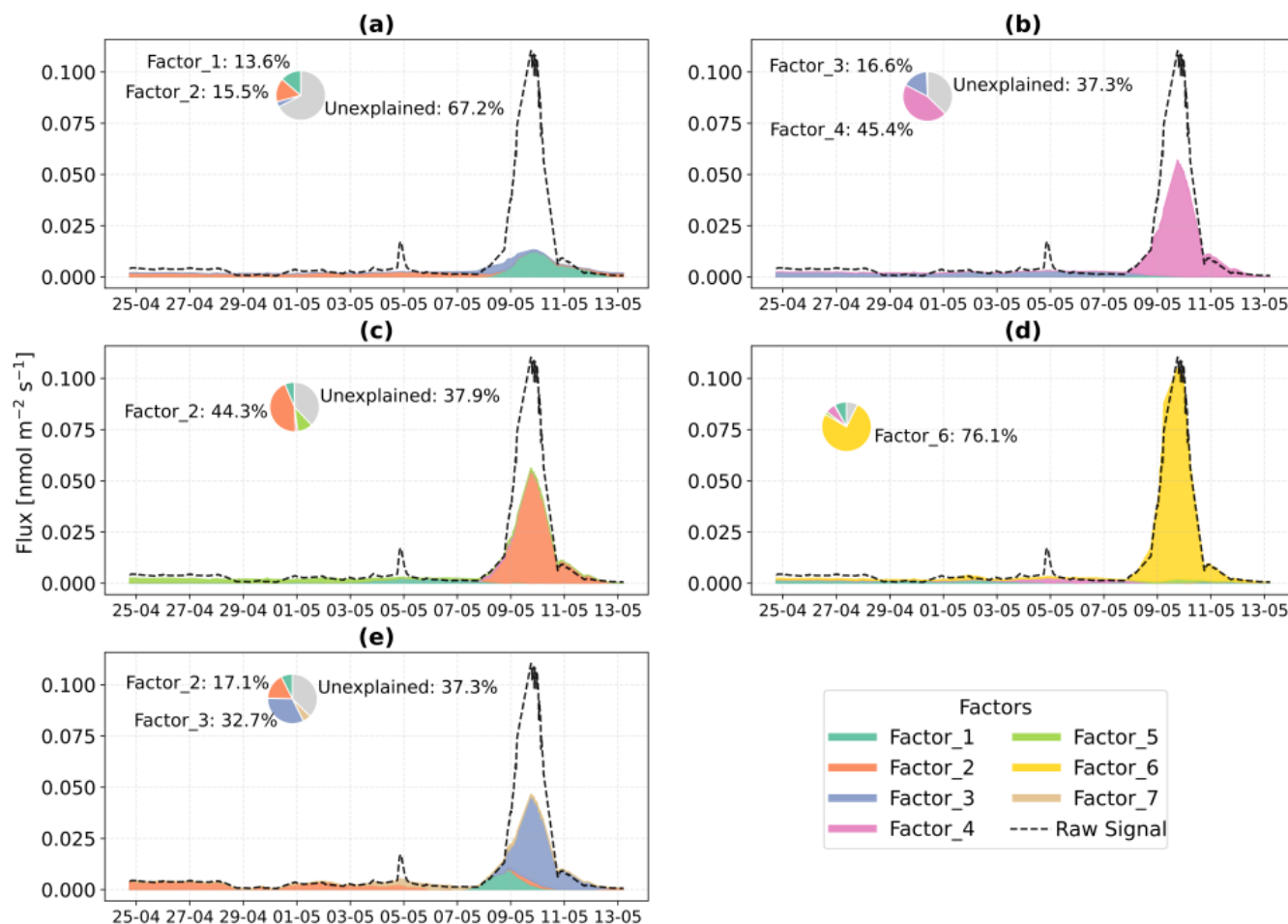
Figure B3. Stacked sesquiterpenes time series showing PMF-resolved factor contributions for 3-factor (a) to 7-factor (e) solutions in Oak. Each subplot represents a different PMF solution. Colored areas correspond to contributions from individual factors, while the white area under the curve indicates unexplained. Inset pie charts represents the total contribution of each factor to the sesquiterpenes signal.
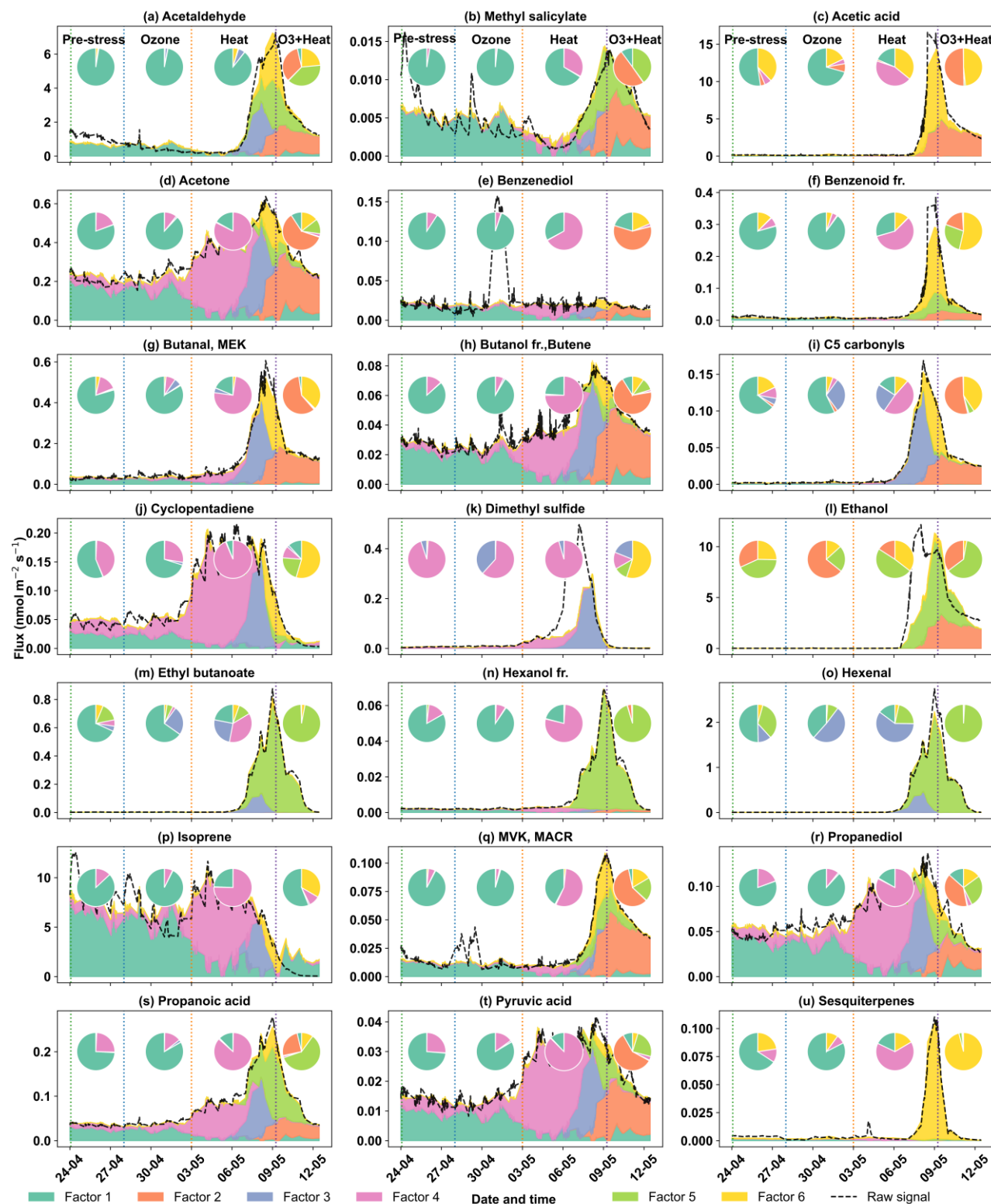
Figure B4. Stacked time series of PMF-resolved contributions for selected BVOC compounds during the Oak experiment. The black dashed lines indicate the original concentration of specific compounds, while stacked colored areas represent contributions from the
740 **six PMF-resolved factors. Each compound's emission is displayed across the four stress periods (Pre-stress, O₃ stress, O₃ + Heat stress, Heat stress), separated by vertical dashed lines. Inset pie charts show the relative contribution of each factor to compound emissions within each stress period, as a factor dominance.**

Data and materials availability

The data and code used in this study are currently available at https://github.com/biplobforestry/Stress_BVOC_Fingerprints.
745 They are in the process of being archived in the Jülich Data repository. The final dataset and code will be assigned a DOI and made publicly available before publication.

Author contribution

E.Y.P., R.R., and T.H. conceptualized the study. B.D was responsible for data analysis, software, visualization, and writing original draft. PTR measurements were performed by E.Y.P. and Y.W. GC measurements were carried out by T.D.S. and R.R.
750 T.H. was responsible for the chamber system. Validation was performed by E.Y.P. (data calibration including all analysis), P.K. and G.I.G. (Positive Matrix Factorization), and M.S. and S.V. (Machine Learning). R.R. and E.Y.P. secured funding. The study was supervised by E.Y.P. and A.K. All authors contributed to writing and revising the manuscript, and they approved the final version.

Competing interests

755 The authors have no other competing interests to declare.

Acknowledgements

The authors would like to thank Mark Müller-Linow for guidance on measuring leaf area index, and Beate Uhlig and Katharina Wolter-Heinen for support in maintaining trees in the greenhouse. We also acknowledge Beatrix Kammer, Niklas Ruland, Christoph Küpper, Benjamin Winter and Sergej Wedel for technical and logistical help with the plant chamber and instruments,
760 Joseph Donald Martin for assistance with the analysis of sorbent tubes and Andrea Carolina Marcillo Lara for verifying the calibration standard composition.

Financial support

This research was supported by an ATMO-ACCESS TNA grant (ATMO-TNA-5G-0000000106). E.Y.P. was funded by a Feodor Lynen Return Fellowship from the Alexander von Humboldt Foundation. R.R. and T.D.S. were supported by the

765 Danish National Research Foundation (DNRF168). B.D. acknowledges support through a DAAD-EPOS (Deutscher Akademischer Austauschdienst) scholarship.

References

Arneth, A., Harrison, S. P., Zaehle, S., Tsigaridis, K., Menon, S., Bartlein, P. J., Feichter, J., Korhola, A., Kulmala, M., O'Donnell, D., Schurgers, G., Sorvari, S., and Vesala, T.: Terrestrial biogeochemical feedbacks in the climate system, Nat.

770 Geosci., 3, 525–532, https://doi.org/10.1038/ngeo905, 2010.

Baier, M., Kandlbinder, A., Golldack, D., and Dietz, K. J.: Oxidative stress and ozone: perception, signalling and response, Plant. Cell Environ., 28, 1012–1020, https://doi.org/10.1111/J.1365-3040.2005.01326.X, 2005.

Bao, X., Zhou, W., Xu, L., and Zheng, Z.: A meta-analysis on plant volatile organic compound emissions of different plant species and responses to environmental stress, Environ. Pollut., 318, 120886,

775 https://doi.org/10.1016/J.ENVPOL.2022.120886, 2023.

Basile, A., Badalamenti, N., Postiglione, A., Shan, Y., and Jin, S.: Biosynthetic Machinery to Abiotic Stress-Driven Emission: Decoding Multilayer Regulation of Volatile Terpenoids in Plants, Antioxidants 2025, Vol. 14, Page 673, 14, 673, https://doi.org/10.3390/ANTIOX14060673, 2025.

Bergman, M. E., Kortbeek, R. W. J., Gutensohn, M., and Dudareva, N.: Plant terpenoid biosynthetic network and its multiple

780 layers of regulation, Prog. Lipid Res., 95, 101287, https://doi.org/10.1016/J.PLIPRES.2024.101287, 2024.

Bhattu, D., Tripathi, S. N., Bhowmik, H. S., Moschos, V., Lee, C. P., Rauber, M., Salazar, G., Abbaszade, G., Cui, T., Slowik, J. G., Vats, P., Mishra, S., Lalchandani, V., Satish, R., Rai, P., Casotto, R., Tobler, A., Kumar, V., Hao, Y., Qi, L., Khare, P., Manousakas, M. I., Wang, Q., Han, Y., Tian, J., Darfeuil, S., Minguillon, M. C., Hueglin, C., Conil, S., Rastogi, N., Srivastava, A. K., Ganguly, D., Bjelic, S., Canonaco, F., Schnelle-Kreis, J., Dominutti, P. A., Jaffrezo, J. L., Szidat, S., Chen, Y., Cao, J.,

785 Baltensperger, U., Uzu, G., Daellenbach, K. R., El Haddad, I., and Prévôt, A. S. H.: Local incomplete combustion emissions define the PM2.5 oxidative potential in Northern India, Nat. Commun., 15, 1–13, https://doi.org/10.1038/S41467-024-47785-5, 2024.

Birami, B., Bamberger, I., Ghirardo, A., Grote, R., Arneth, A., Gaona-Colmán, E., Nadal-Sala, D., and Ruehr, N. K.: Heatwave frequency and seedling death alter stress-specific emissions of volatile organic compounds in Aleppo pine, Oecologia 2021

790 1974, 197, 939–956, https://doi.org/10.1007/S00442-021-04905-Y, 2021.

Bourtsoukidis, E., Bonn, B., Dittmann, A., Hakola, H., Hellén, H., and Jacobi, S.: Ozone stress as a driving force of sesquiterpene emissions: a suggested parameterisation, Biogeosciences, 9, 4337–4352, https://doi.org/10.5194/bg-9-4337-2012, 2012.

Brilli, F., Ruuskanen, T. M., Schnitzhofer, R., Müller, M., Breitenlechner, M., Bittner, V., Wohlfahrt, G., Loreto, F., and

795 Hansel, A.: Detection of Plant Volatiles after Leaf Wounding and Darkening by Proton Transfer Reaction "Time-of-Flight" Mass Spectrometry (PTR-TOF), PLoS One, 6, e20419, https://doi.org/10.1371/JOURNAL.PONE.0020419, 2011.

Cappellin, L., Karl, T., Probst, M., Ismailova, O., Winkler, P. M., Soukoulis, C., Aprea, E., Märk, T. D., Gasperi, F., and Biasioli, F.: On quantitative determination of volatile organic compound concentrations using proton transfer reaction time-of-flight mass spectrometry, Environ. Sci. Technol., 46, 2283–2290, https://doi.org/10.1021/ES203985T, 2012.

800   Cappellin, L., Loreto, F., Biasioli, F., Pastore, P., and McKinney, K.: A mechanism for biogenic production and emission of MEK from MVK decoupled from isoprene biosynthesis, Atmos. Chem. Phys., 19, 3125–3135, https://doi.org/10.5194/ACP-19-3125-2019, 2019.

Di Carlo, P., Brune, W. H., Martinez, M., Harder, H., Lesher, R., Ren, X., Thornberry, T., Carroll, M. A., Young, V., Shepson, P. B., Riemer, D., Apel, E., and Campbell, C.: Missing OH Reactivity in a Forest: Evidence for Unknown Reactive Biogenic

805   VOCs, Science (80-.)., 304, 722–725, https://doi.org/10.1126/SCIENCE.1094392, 2004.

Churkina, G., Kuik, F., Bonn, B., Lauer, A., Grote, R., Tomiak, K., and Butler, T. M.: Effect of VOC Emissions from Vegetation on Air Quality in Berlin during a Heatwave, Environ. Sci. Technol., 51, 6120–6130, https://doi.org/10.1021/ACS.EST.6B06514, 2017.

Cofer, T. M., Engelberth, M., and Engelberth, J.: Green leaf volatiles protect maize (Zea mays) seedlings against damage from

810   cold stress, Plant. Cell Environ., 41, 1673–1682, https://doi.org/10.1111/PCE.13204, 2018.

Cook, B. I., Mankin, J. S., and Anchukaitis, K. J.: Climate Change and Drought: From Past to Future, Curr. Clim. Chang. Reports 2018 42, 4, 164–179, https://doi.org/10.1007/S40641-018-0093-2, 2018.

Daussy, J. and Staudt, M.: Do future climate conditions change volatile organic compound emissions from Artemisia annua? Elevated CO2 and temperature modulate actual VOC emission rate but not its emission capacity, Atmos. Environ. X, 7,

815   100082, https://doi.org/10.1016/j.aeaoa.2020.100082, 2020.

Davison, B., Brunner, A., Ammann, C., Spirig, C., Jocher, M., and Neftel, A.: Cut-induced VOC emissions from agricultural grasslands, Plant Biol., 10, 76–85, https://doi.org/10.1055/S-2007-965043, 2008.

Dicke, M. and Baldwin, I. T.: The evolutionary context for herbivore-induced plant volatiles: beyond the 'cry for help,' Trends Plant Sci., 15, 167–175, https://doi.org/10.1016/J.TPLANTS.2009.12.002, 2010.

820   Dizengremel, P., Le Thiec, D., Bagard, M., and Jolivet, Y.: Ozone risk assessment for plants: Central role of metabolism-dependent changes in reducing power, Environ. Pollut., 156, 11–15, https://doi.org/10.1016/J.ENVPOL.2007.12.024, 2008.

Edtbauer, A., Pfannerstill, E. Y., Pires Florentino, A. P., Barbosa, C. G. G., Rodriguez-Caballero, E., Zannoni, N., Alves, R. P., Wolff, S., Tsokankunku, A., Aptroot, A., de Oliveira Sá, M., de Araújo, A. C., Sörgel, M., de Oliveira, S. M., Weber, B., and Williams, J.: Cryptogamic organisms are a substantial source and sink for volatile organic compounds in the Amazon

825   region, Commun. Earth Environ. 2021 21, 2, 1–14, https://doi.org/10.1038/s43247-021-00328-y, 2021.

Feng, Z., Yuan, X., Fares, S., Loreto, F., Li, P., Hoshika, Y., and Paoletti, E.: Isoprene is more affected by climate drivers than monoterpenes: A meta-analytic review on plant isoprenoid emissions, Plant. Cell Environ., 42, 1939–1949, https://doi.org/10.1111/PCE.13535, 2019.

Feng, Z., Agathokleous, E., Yue, X., Oksanen, E., Paoletti, E., Sase, H., Gandin, A., Koike, T., Calatayud, V., Yuan, X., Liu,

830   X., De Marco, A., Jolivet, Y., Kontunen-Soppela, S., Hoshika, Y., Saji, H., Li, P., Li, Z., Watanabe, M., and Kobayashi, K.:

Emerging challenges of ozone impacts on asian plants: actions are needed to protect ecosystem health, Ecosyst. Heal. Sustain., 7, https://doi.org/10.1080/20964129.2021.1911602, 2021.

Fineschi, S., Loreto, F., Staudt, M., and Peñuelas, J.: Diversification of Volatile Isoprenoid Emissions from Trees: Evolutionary and Ecological Perspectives, 1–20, https://doi.org/10.1007/978-94-007-6606-8_1, 2013.

835 Fitzky, A. C., Sandén, H., Karl, T., Fares, S., Calfapietra, C., Grote, R., Saunier, A., and Rewald, B.: The Interplay Between Ozone and Urban Vegetation—BVOC Emissions, Ozone Deposition, and Tree Ecophysiology, Front. For. Glob. Chang., 2, 476346, https://doi.org/10.3389/FFGC.2019.00050, 2019.

Fitzky, A. C., Kaser, L., Peron, A., Karl, T., Graus, M., Tholen, D., Halbwirth, H., Trimmel, H., Pesendorfer, M., Rewald, B., and Sandén, H.: Same, same, but different: Drought and salinity affect BVOC emission rate and alter blend composition of
840 urban trees, Urban For. Urban Green., 80, 0–2, https://doi.org/10.1016/j.ufug.2023.127842, 2023.

Furnell, H., Wenger, J., Wingler, A., Kilcawley, K. N., Mannion, D. T., Skibinska, I., and Kammer, J.: Highly diverse emission of volatile organic compounds by Sitka spruce and determination of their emission pathways, Environ. Sci. Atmos., 5, 242–260, https://doi.org/10.1039/D4EA00138A, 2025.

Gaucher, C., Costanzo, N., Widden, P., Renaud, J. P., Dizengremel, P., Mauffette, Y., and Chevrier, N.: Response to an ozone
845 gradient of growth and enzymes implicated in tolerance to oxidative stress in Acer saccharum (Marsh.) seedlings, Ann. For. Sci., 63, 387–397, https://doi.org/10.1051/forest:2006019, 2006.

Genard-Zielinski, A. C., Boissard, C., Ormeño, E., Lathière, J., Reiter, I. M., Wortham, H., Orts, J. P., Temime-Roussel, B., Guenet, B., Bartsch, S., Gauquelin, T., and Fernandez, C.: Seasonal variations of Quercus pubescens isoprene emissions from an in natura forest under drought stress and sensitivity to future climate change in the Mediterranean area, Biogeosciences, 15,
850 4711–4730, https://doi.org/10.5194/BG-15-4711-2018, 2018.

Gkatzelis, G. I., Coggon, M. M., McDonald, B. C., Peischl, J., Gilman, J. B., Aikin, K. C., Robinson, M. A., Canonaco, F., Prevot, A. S. H., Trainer, M., and Warneke, C.: Observations Confirm that Volatile Chemical Products Are a Major Source of Petrochemical Emissions in U.S. Cities, Environ. Sci. Technol., 55, 4332–4343, https://doi.org/10.1021/ACS.EST.0C05471/ASSET/IMAGES/LARGE/ES0C05471_0005.JPEG, 2021.

855 Graham, J. L., Staudt, M., Buatois, B., and Caro, S. P.: Developing Oak Buds Produce Volatile Emissions in Response to Herbivory by Freshly Hatched Caterpillars, J. Chem. Ecol., 50, 503–514, https://doi.org/10.1007/S10886-024-01520-Y, 2024.

Guenther, A. B., Zimmerman, P. R., Harley, P. C., Monson, R. K., and Fall, R.: Isoprene and monoterpene emission rate variability: Model evaluations and sensitivity analyses, J. Geophys. Res. Atmos., 98, 12609–12617, https://doi.org/10.1029/93JD00527, 1993.

860 Guenther, A. B., Jiang, X., Heald, C. L., Sakulyanontvittaya, T., Duhl, T., Emmons, L. K., and Wang, X.: The Model of Emissions of Gases and Aerosols from Nature version 2.1 (MEGAN2.1): an extended and updated framework for modeling biogenic emissions, Geosci. Model Dev., 5, 1471–1492, https://doi.org/10.5194/gmd-5-1471-2012, 2012.

Guo, C., Wang, X., Wang, Q., Zhao, Z., Xie, B., Xu, L., and Zhang, R.: Plant defense mechanisms against ozone stress: Insights from secondary metabolism, Environ. Exp. Bot., 217, 105553, https://doi.org/10.1016/J.ENVEXPBOT.2023.105553, 2024.

865   Heil, M. and Karban, R.: Explaining evolution of plant communication by airborne signals., Trends Ecol. Evol., 25, 137–144, https://doi.org/10.1016/j.tree.2009.09.010, 2010.

Hertig, E., Russo, A., and Trigo, R. M.: Heat and Ozone Pollution Waves in Central and South Europe—Characteristics, Weather Types, and Association with Mortality, Atmos. 2020, Vol. 11, Page 1271, 11, 1271, https://doi.org/10.3390/ATMOS11121271, 2020.

870   Hohaus, T., Kuhn, U., Andres, S., Kaminski, M., Rohrer, F., Tillmann, R., Wahner, A., Wegener, R., Yu, Z., and Kiendler-Scharr, A.: A new plant chamber facility, PLUS, coupled to the atmosphere simulation chamber SAPHIR, Atmos. Meas. Tech., 9, 1247–1259, https://doi.org/10.5194/amt-9-1247-2016, 2016.

Holopainen, J. K., Virjamo, V., Ghimire, R. P., Blande, J. D., Julkunen-Tiitto, R., and Kivimäenpää, M.: Climate Change Effects on Secondary Compounds of Forest Trees in the Northern Hemisphere, Front. Plant Sci., 9, 1–10,
875   https://doi.org/10.3389/fpls.2018.01445, 2018.

IPCC: Summary for Policymakers: Synthesis Report., Clim. Chang. 2023 Synth. Report. Contrib. Work. Groups I, II III to Sixth Assess. Rep. Intergov. Panel Clim. Chang., 1–34, https://doi.org/10.59327/IPCC/AR6-9789291691647.001, 2023.

Iwasa, Y., Hayashi, R., and Satake, A.: Optimal seasonal schedule for the production of isoprene, a highly volatile biogenic VOC, Sci. Rep., 14, 1–10, https://doi.org/10.1038/S41598-024-62975-3, 2024.

880   Jandl, R., Kirchmeir, H., Liepin, K., and Bleive, A.: The Potential of European Beech (Fagus sylvatica L.) in the Hemiboreal Baltic Region: A Review, For. 2025, Vol. 16, Page 109, 16, 109, https://doi.org/10.3390/F16010109, 2025.

Jardine, K. J., Chambers, J. Q., Holm, J., Jardine, A. B., Fontes, C. G., Zorzanelli, R. F., Meyers, K. T., de Souza, V. F., Garcia, S., Gimenez, B. O., Piva, L. R. d. O., Higuchi, N., Artaxo, P., Martin, S., and Manzi, A. O.: Green Leaf Volatile Emissions during High Temperature and Drought Stress in a Central Amazon Rainforest, Plants, 4, 678,
885   https://doi.org/10.3390/PLANTS4030678, 2015.

Jardine, K. J., Jardine, A. B., Holm, J. A., Lombardozzi, D. L., Negron-Juarez, R. I., Martin, S. T., Beller, H. R., Gimenez, B. O., Higuchi, N., and Chambers, J. Q.: Monoterpene 'thermometer' of tropical forest-atmosphere response to climate warming, Plant. Cell Environ., 40, 441–452, https://doi.org/10.1111/PCE.12879, 2017.

Jensen, A. R., Koss, A. R., Hales, R. B., and De Gouw, J. A.: Measurements of volatile organic compounds in ambient air by
890   gas-chromatography and real-Time Vocus PTR-TOF-MS: Calibrations, instrument background corrections, and introducing a PTR Data Toolkit, Atmos. Meas. Tech., 16, 5261–5285, https://doi.org/10.5194/AMT-16-5261-2023, 2023.

Jiang, J., Aksoyoglu, S., Ciarelli, G., Oikonomakis, E., El-Haddad, I., Canonaco, F., O'Dowd, C., Ovadnevaite, J., Minguillón, M. C., Baltensperger, U., and Prévôt, A. S. H.: Effects of two different biogenic emission models on modelled ozone and aerosol concentrations in Europe, Atmos. Chem. Phys., 19, 3747–3768, https://doi.org/10.5194/acp-19-3747-2019, 2019.

895   Kangasjärvi, J., Jaspers, P., and Kollist, H.: Signalling and cell death in ozone-exposed plants, Plant. Cell Environ., 28, 1021–1036, https://doi.org/10.1111/J.1365-3040.2005.01325.X, 2005.

Karl, M., Guenther, A., Köble, R., Leip, A., and Seufert, G.: A new European plant-specific emission inventory of biogenic volatile organic compounds for use in atmospheric transport models, Biogeosciences, 6, 1059–1087,

https://doi.org/10.5194/bg-6-1059-2009, 2009.

900   Karnosky, D. F., Skelly, J. M., Percy, K. E., and Chappelka, A. H.: Perspectives regarding 50 years of research on effects of tropospheric ozone air pollution on US forests, Environ. Pollut., 147, 489–506, https://doi.org/10.1016/J.ENVPOL.2006.08.043, 2007.

Khalaj, F., Rivas-Ubach, A., Anderton, C. R., China, S., Mooney, K., and Faiola, C. L.: Acyclic Terpenes Reduce Secondary Organic Aerosol Formation from Emissions of a Riparian Shrub, ACS Earth Sp. Chem., 5, 1242–1253,

905   https://doi.org/10.1021/ACSEARTHSPACECHEM.0C00300, 2021.

Kivimäenpää, M., Riikonen, J., Ahonen, V., Tervahauta, A., and Holopainen, T.: Sensitivity of Norway spruce physiology and terpenoid emission dynamics to elevated ozone and elevated temperature under open-field exposure, Environ. Exp. Bot., 90, 32–42, https://doi.org/10.1016/J.ENVEXPBOT.2012.11.004, 2013.

Kivimäenpää, M., Ghimire, R. P., Sutinen, S., Häikiö, E., Kasurinen, A., Holopainen, T., and Holopainen, J. K.: Increases in

910   volatile organic compound emissions of Scots pine in response to elevated ozone and warming are modified by herbivory and soil nitrogen availability, Eur. J. For. Res., 135, 343–360, https://doi.org/10.1007/s10342-016-0939-x, 2016.

Kleist, E., Mentel, T. F., Andres, S., Bohne, A., Folkers, A., Kiendler-Scharr, A., Rudich, Y., Springer, M., Tillmann, R., and Wildt, J.: Impact of heat stress on the emissions of monoterpenes, sesquiterpenes, phenolic BVOC and green leaf volatiles from several tree species, https://doi.org/10.5194/bgd-9-9533-2012, 2012a.

915   Kleist, E., Mentel, T. F., Andres, S., Bohne, A., Folkers, A., Kiendler-Scharr, A., Rudich, Y., Springer, M., Tillmann, R., and Wildt, J.: Irreversible impacts of heat on the emissions of monoterpenes, sesquiterpenes, phenolic BVOC and green leaf volatiles from several tree species, Biogeosciences, 9, 5111–5123, https://doi.org/10.5194/bg-9-5111-2012, 2012b.

Krechmer, J., Lopez-Hilfiker, F., Koss, A., Hutterli, M., Stoermer, C., Deming, B., Kimmel, J., Warneke, C., Holzinger, R., Jayne, J., Worsnop, D., Fuhrer, K., Gonin, M., and De Gouw, J.: Evaluation of a New Reagent-Ion Source and Focusing Ion-

920   Molecule Reactor for Use in Proton-Transfer-Reaction Mass Spectrometry, Anal. Chem., 90, 12011–12018, https://doi.org/10.1021/ACS.ANALCHEM.8B02641, 2018.

Kutty, N. N. and Mishra, M.: Dynamic distress calls: volatile info chemicals induce and regulate defense responses during herbivory, Front. Plant Sci., 14, 1–16, https://doi.org/10.3389/fpls.2023.1135000, 2023.

Li, Z., Ratliff, E. A., and Sharkey, T. D.: Effect of Temperature on Postillumination Isoprene Emission in Oak and Poplar,

925   Plant Physiol., 155, 1037, https://doi.org/10.1104/PP.110.167551, 2010.

Liu, B., Kaurilind, E., Zhang, L., Okereke, C. N., Remmel, T., and Niinemets, Ü.: Improved plant heat shock resistance is introduced differently by heat and insect infestation: the role of volatile emission traits, Oecologia, 199, 53–68, https://doi.org/10.1007/S00442-022-05168-X, 2022.

Lõpez, M. A., Vicente, J., Kulasekaran, S., Vellosillo, T., Martínez, M., Irigoyen, M. L., Cascõn, T., Bannenberg, G., Hamberg,

930   M., and Castresana, C.: Antagonistic role of 9-lipoxygenase-derived oxylipins and ethylene in the control of oxidative stress, lipid peroxidation and plant defence, Plant J., 67, 447–458, https://doi.org/10.1111/J.1365-313X.2011.04608.X, 2011.

Loreto, F. and Schnitzler, J. P.: Abiotic stresses and induced BVOCs, Trends Plant Sci., 15, 154–166,

https://doi.org/10.1016/J.TPLANTS.2009.12.006, 2010.

Loreto, F., Pinelli, P., Manes, F., and Kollist, H.: Impact of ozone on monoterpene emissions and evidence for an isoprene-like antioxidant action of monoterpenes emitted by Quercus ilex leaves, Tree Physiol., 24, 361–367, https://doi.org/10.1093/TREEPHYS/24.4.361, 2004.

Loubet, B., Buysse, P., Gonzaga-Gomez, L., Lafouge, F., Ciuraru, R., Decuq, C., Kammer, J., Bsaibes, S., Boissard, C., Durand, B., Gueudet, J. C., Fanucci, O., Zurfluh, O., Abis, L., Zannoni, N., Truong, F., Baisnée, D., Sarda-Estève, R., Staudt, M., and Gros, V.: Volatile organic compound fluxes over a winter wheat field by PTR-Qi-TOF-MS and eddy covariance, Atmos. Chem. Phys., 22, 2817–2842, https://doi.org/10.5194/ACP-22-2817-2022, 2022.

Lundberg, S. M. and Lee, S. I.: A Unified Approach to Interpreting Model Predictions, Adv. Neural Inf. Process. Syst., 2017-December, 4766–4775, 2017.

Maison, A., Lugon, L., Park, S. J., Baudic, A., Cantrell, C., Couvidat, F., D'Anna, B., Di Biagio, C., Gratien, A., Gros, V., Kalalian, C., Kammer, J., Michoud, V., Petit, J. E., Shahin, M., Simon, L., Valari, M., Vigneron, J., Tuzet, A., and Sartelet, K.: Significant impact of urban tree biogenic emissions on air quality estimated by a bottom-up inventory and chemistry transport modeling, Atmos. Chem. Phys., 24, 6011–6046, https://doi.org/10.5194/ACP-24-6011-2024, 2024.

Van Meeningen, Y., Schurgers, G., Rinnan, R., and Holst, T.: BVOC emissions from English oak (Quercus robur) and European beech (Fagus sylvatica) along a latitudinal gradient, Biogeosciences, 13, 6067–6080, https://doi.org/10.5194/bg-13-6067-2016, 2016.

Van Meeningen, Y., Schurgers, G., Rinnan, R., and Holst, T.: Isoprenoid emission response to changing light conditions of English oak, European beech and Norway spruce, Biogeosciences, 14, 4045–4060, https://doi.org/10.5194/bg-14-4045-2017, 2017.

Moukhtar, S., Bessagnet, B., Rouil, L., and Simon, V.: Monoterpene emissions from Beech (Fagus sylvatica) in a French forest and impact on secondary pollutants formation at regional scale, Atmos. Environ., 39, 3535–3547, https://doi.org/10.1016/j.atmosenv.2005.02.031, 2005.

Nagalingam, S., Seco, R., Kim, S., and Guenther, A.: Heat stress strongly induces monoterpene emissions in some plants with specialized terpenoid storage structures, Agric. For. Meteorol., 333, 109400, https://doi.org/10.1016/J.AGRFORMET.2023.109400, 2023.

Niinemets, Ü., Arneth, A., Kuhn, U., Monson, R. K., Peñuelas, J., and Staudt, M.: The emission factor of volatile isoprenoids: Stress, acclimation, and developmental responses, Biogeosciences, 7, 2203–2223, https://doi.org/10.5194/BG-7-2203-2010, 2010.

Nogués, I., Brilli, F., and Loreto, F.: Dimethylallyl Diphosphate and Geranyl Diphosphate Pools of Plant Species Characterized by Different Isoprenoid Emissions, Plant Physiol., 141, 721–730, https://doi.org/10.1104/PP.105.073213, 2006.

Palm, B. B., de Sá, S. S., Day, D. A., Campuzano-Jost, P., Hu, W., Seco, R., Sjostedt, S. J., Park, J.-H., Guenther, A. B., Kim, S., Brito, J., Wurm, F., Artaxo, P., Thalman, R., Wang, J., Yee, L. D., Wernis, R., Isaacman-VanWertz, G., Goldstein, A. H., Liu, Y., Springston, S. R., Souza, R., Newburn, M. K., Alexander, M. L., Martin, S. T., and Jimenez, J. L.: Secondary organic

aerosol formation from ambient air in an oxidation flow reactor in central Amazonia, Atmos. Chem. Phys., 18, 467–493, https://doi.org/10.5194/acp-18-467-2018, 2018.

Paoletti, E.: Ozone and urban forests in Italy, Environ. Pollut., 157, 1506–1512, https://doi.org/10.1016/j.envpol.2008.09.019, 2009.

Pecl, G. T., Araújo, M. B., Bell, J. D., Blanchard, J., Bonebrake, T. C., Chen, I.-C., Clark, T. D., Colwell, R. K., Danielsen, F., Evengård, B., Falconi, L., Ferrier, S., Frusher, S., Garcia, R. A., Griffis, R. B., Hobday, A. J., Janion-Scheepers, C., Jarzyna, M. A., Jennings, S., Lenoir, J., Linnetved, H. I., Martin, V. Y., McCormack, P. C., McDonald, J., Mitchell, N. J., Mustonen, T., Pandolfi, J. M., Pettorelli, N., Popova, E., Robinson, S. A., Scheffers, B. R., Shaw, J. D., Sorte, C. J. B., Strugnell, J. M., Sunday, J. M., Tuanmu, M.-N., Vergés, A., Villanueva, C., Wernberg, T., Wapstra, E., and Williams, S. E.: Biodiversity redistribution under climate change: Impacts on ecosystems and human well-being, Science (80-.)., 355, eaai9214, https://doi.org/10.1126/science.aai9214, 2017.

Pedregosa, F., Varoquaux, G., Gramfort, A., Michel, V., Thirion, B., Grisel, O., Blondel, M., Prettenhofer, P., Weiss, R., Dubourg, V., Vanderplas, J., Passos, A., Cournapeau, D., Brucher, M., Perrot, M., and Duchesnay, É.: Scikit-learn: Machine Learning in Python, J. Mach. Learn. Res., 12, 2825–2830, 2012.

Pelloux, J., Jolivet, Y., Fontaine, V., Banvoy, J., and Dizengremel, P.: Changes in Rubisco and Rubisco activase gene expression and polypeptide content in Pinus halepensis M. subjected to ozone and drought, Plant. Cell Environ., 24, 123–131, https://doi.org/10.1046/J.1365-3040.2001.00665.X, 2001.

Peñuelas, J. and Llusià, J.: Plant VOC emissions: making use of the unavoidable, Trends Ecol. Evol., 19, 402–404, https://doi.org/10.1016/j.tree.2004.06.002, 2004.

Peñuelas, J. and Munné-Bosch, S.: Isoprenoids: An evolutionary pool for photoprotection, Trends Plant Sci., 10, 166–169, https://doi.org/10.1016/j.tplants.2005.02.005, 2005.

Peron, A., Kaser, L., Charlott Fitzky, A., Graus, M., Halbwirth, H., Greiner, J., Wohlfahrt, G., Rewald, B., Sandén, H., and Karl, T.: Combined effects of ozone and drought stress on the emission of biogenic volatile organic compounds from Quercus robur L., Biogeosciences, 18, 535–556, https://doi.org/10.5194/bg-18-535-2021, 2021.

Pfannerstill, E. Y., Arata, C., Zhu, Q., Schulze, B. C., Woods, R., Seinfeld, J. H., Bucholtz, A., Cohen, R. C., and Goldstein, A. H.: Volatile organic compound fluxes in the agricultural San Joaquin Valley - Spatial distribution, source attribution, and inventory comparison, Atmos. Chem. Phys., 23, 12753–12780, https://doi.org/10.5194/ACP-23-12753-2023, 2023.

Pfannerstill, E. Y., Arata, C., Zhu, Q., Schulze, B. C., Ward, R., Woods, R., Harkins, C., Schwantes, R. H., Seinfeld, J. H., Bucholtz, A., Cohen, R. C., and Goldstein, A. H.: Temperature-dependent emissions dominate aerosol and ozone formation in Los Angeles, Science, 384, 1324–1329, https://doi.org/10.1126/SCIENCE.ADG8204, 2024.

Pikkarainen, L., Nissinen, K., Ghimire, R. P., Kivimäenpää, M., Ikonen, V.-P., Kilpeläinen, A., Virjamo, V., Yu, H., Kirsikka-Aho, S., Salminen, T., Hirvonen, J., Vahimaa, T., Luoranen, J., and Peltola, H.: Responses in growth and emissions of biogenic volatile organic compounds in Scots pine, Norway spruce and silver birch seedlings to different warming treatments in a controlled field experiment, Sci. Total Environ., 821, 153277, https://doi.org/10.1016/j.scitotenv.2022.153277, 2022.

Pinto, D. M., Blande, J. D., Souza, S. R., Nerg, A. M., and Holopainen, J. K.: Plant volatile organic compounds (VOCs) in ozone (O3) polluted atmospheres: the ecological effects, J. Chem. Ecol., 36, 22–34, https://doi.org/10.1007/S10886-009-9732-3, 2010.

Pugliese, G., Ingrisch, J., Meredith, L. K., Pfannerstill, E. Y., Klüpfel, T., Meeran, K., Byron, J., Purser, G., Gil-Loaiza, J., van Haren, J., Dontsova, K., Kreuzwieser, J., Ladd, S. N., Werner, C., and Williams, J.: Effects of drought and recovery on soil volatile organic compound fluxes in an experimental rainforest, Nat. Commun., 14, 5064, https://doi.org/10.1038/s41467-023-40661-8, 2023.

Quintanilla-Casas, B., Bro, R., Hinrich, J. L., and Davie-Martin, C. L.: Tutorial on PARADISe: PARAFAC2-based Deconvolution and Identification System for processing GC–MS data, https://doi.org/10.21203/RS.3.PEX-2143/V1, 2023.

Raftoyannis, Y. and Radoglou, K.: Physiological Responses of Beech and Sessile Oak in a Natural Mixed Stand During a Dry Summer, Ann. Bot., 89, 723, https://doi.org/10.1093/AOB/MCF133, 2002.

Renaut, J., Bohler, S., Hausman, J. F., Hoffmann, L., Sergeant, K., Ahsan, N., Jolivet, Y., and Dizengremel, P.: The impact of atmospheric composition on plants: A case study of ozone and poplar, Mass Spectrom. Rev., 28, 495–516, https://doi.org/10.1002/MAS.20202, 2009.

Rieksta, J., Li, T., Davie-Martin, C. L., Aeppli, L. C. B., Høye, T. T., and Rinnan, R.: Volatile responses of dwarf birch to mimicked insect herbivory and experimental warming at two elevations in Greenlandic tundra, Plant-Environment Interact., 4, 23–35, https://doi.org/10.1002/PEI3.10100, 2023.

Rinnan, R., Iversen, L. L., Tang, J., Vedel-Petersen, I., Schollert, M., and Schurgers, G.: Separating direct and indirect effects of rising temperatures on biogenic volatile emissions in the Arctic, Proc. Natl. Acad. Sci. U. S. A., 117, 32476–32483, https://doi.org/10.1073/PNAS.2008901117, 2020.

Roy, S., Kapoor, R., and Mathur, P.: Revisiting Changes in Growth, Physiology and Stress Responses of Plants under the Effect of Enhanced CO2 and Temperature, Plant Cell Physiol., 65, 4–19, https://doi.org/10.1093/PCP/PCAD121, 2024.

Royal Society: Ground-level ozone in the 21st century: future trends, impacts and policy implications, 134 pp., 2008.

Schneider, C. A., Rasband, W. S., and Eliceiri, K. W.: NIH Image to ImageJ: 25 years of image analysis, Nat. Methods 2012 97, 9, 671–675, https://doi.org/10.1038/nmeth.2089, 2012.

Sharkey, T. D.: Effects of moderate heat stress on photosynthesis: importance of thylakoid reactions, rubisco deactivation, reactive oxygen species, and thermotolerance provided by isoprene, Plant. Cell Environ., 28, 269–277, https://doi.org/10.1111/J.1365-3040.2005.01324.X, 2005.

Sharkey, T. D., Chen, X., and Yeh, S.: Isoprene Increases Thermotolerance of Fosmidomycin-Fed Leaves, Plant Physiol., 125, 2001, https://doi.org/10.1104/PP.125.4.2001, 2001.

Sindelarova, K., Granier, C., Bouarar, I., Guenther, A., Tilmes, S., Stavrakou, T., Müller, J.-F., Kuhn, U., Stefani, P., and Knorr, W.: Global data set of biogenic VOC emissions calculated by the MEGAN model over the last 30 years, Atmos. Chem. Phys., 14, 9317–9341, https://doi.org/10.5194/acp-14-9317-2014, 2014.

Singsaas, E. L.: Terpenes and the thermotolerance of photosynthesis, New Phytol., 146, 1–4, https://doi.org/10.1046/J.1469-

1035 8137.2000.00626.X, 2000.

Song, J., Gkatzelis, G. I., Tillmann, R., Brüggemann, N., Leisner, T., and Saathoff, H.: Characterization of biogenic volatile organic compounds and their oxidation products at a stressed pine forest close to a biogas power plant, https://doi.org/10.5194/EGUSPHERE-2024-1768, 2024.

Szopa, S., Naik, V., Adhikary, B., Artaxo, P., Berntsen, T., Collins, W. D., Fuzzi, S., Gallardo, L., Kiendler-Scharr, A.,

1040 Klimont, Z., Liao, H., Unger, N., and Zanis, P.: Short-Lived Climate Forcers, in: Climate Change 2021: The Physical Science Basis. Contribution of Working Group I to the Sixth Assessment Report of the Intergovernmental Panel on Climate Change, edited by: Masson-Delmotte, V., Zhai, P., Pirani, A., Connors, S. L., Péan, C., Berger, S., Caud, N., Chen, Y., Goldfarb, L., Gomis, M. I., Huang, M., Leitzell, K., Lonnoy, E., Matthews, J., Maycock, T. K., Waterfield, T., Yelekçi, O., Yu, R., and Zhou, B., Cambridge University Press, Cambridge, United Kingdom and New York, NY, USA, 817–922 pp.,

1045 https://doi.org/10.1017/9781009157896.008, 2021.

Turan, S., Kask, K., Kanagendran, A., Li, S., Anni, R., Talts, E., Rasulov, B., Kännaste, A., and Niinemets, U.: Lethal heat stress-dependent volatile emissions from tobacco leaves: what happens beyond the thermal edge?, J. Exp. Bot., 70, 5017–5030, https://doi.org/10.1093/JXB/ERZ255, 2019.

Vella, R., Pozzer, A., Forrest, M., Lelieveld, J., Hickler, T., and Tost, H.: Changes in biogenic volatile organic compound

1050 emissions in response to the El Niño--Southern Oscillation, Biogeosciences, 20, 4391–4412, https://doi.org/10.5194/bg-20-4391-2023, 2023.

Vo, T. and Faiola, C. L.: Acute ozone exposure decreases terpene emissions from Canary Island pines, Agric. For. Meteorol., 333, 109416, https://doi.org/https://doi.org/10.1016/j.agrformet.2023.109416, 2023.

Werner, C., Fasbender, L., Romek, K. M., Yáñez-Serrano, A. M., and Kreuzwieser, J.: Heat Waves Change Plant Carbon

1055 Allocation Among Primary and Secondary Metabolism Altering CO2 Assimilation, Respiration, and VOC Emissions, Front. Plant Sci., 11, 512788, https://doi.org/10.3389/fpls.2020.01242, 2020.

Wu, Q., Zhang, Z., Zhu, H., Li, T., Zhu, X., Gao, H., Yun, Z., and Jiang, Y.: Comparative volatile compounds and primary metabolites profiling of pitaya fruit peel after ozone treatment, J. Sci. Food Agric., 99, 2610–2621, https://doi.org/10.1002/JSFA.9479, 2019.

1060 Xu, S., Chen, W., Huang, Y., and He, X.: Responses of growth, photosynthesis and VOC emissions of Pinus tabulaeformis Carr. Exposure to elevated CO2 and/or elevated O3 in an urban area, Bull. Environ. Contam. Toxicol., 88, 443–448, https://doi.org/10.1007/S00128-011-0462-1, 2012.

Yang, X., Zeng, G., Iyakaremye, V., and Zhu, B.: Effects of different types of heat wave days on ozone pollution over Beijing-Tianjin-Hebei and its future projection, Sci. Total Environ., 837, 155762, https://doi.org/10.1016/j.scitotenv.2022.155762,

1065 2022.

Yang, Y., Sun, F., Hu, C., Gao, J., Wang, W., Chen, Q., and Ye, J.: Emissions of Biogenic Volatile Organic Compounds from Plants: Impacts of Air Pollutants and Environmental Variables, Curr. Pollut. Reports, 11, 1–18, https://doi.org/10.1007/S40726-024-00339-1, 2025.

Zhu, Q., Schwantes, R. H., Coggon, M., Harkins, C., Schnell, J., He, J., Pye, H. O. T., Li, M., Baker, B., Moon, Z., Ahmadov,
1070   R., Pfannerstill, E. Y., Place, B., Wooldridge, P., Schulze, B. C., Arata, C., Bucholtz, A., Seinfeld, J. H., Warneke, C.,
Stockwell, C. E., Xu, L., Zuraski, K., Robinson, M. A., Neuman, J. A., Veres, P. R., Peischl, J., Brown, S. S., Goldstein, A.
H., Cohen, R. C., and McDonald, B. C.: A better representation of volatile organic compound chemistry in WRF-Chem and
its impact on ozone over Los Angeles, Atmos. Chem. Phys., 24, 5265–5286, https://doi.org/10.5194/ACP-24-5265-2024,
2024.

1075   Zscheischler, J., Martius, O., Westra, S., Bevacqua, E., Raymond, C., Horton, R. M., van den Hurk, B., AghaKouchak, A.,
Jézéquel, A., Mahecha, M. D., Maraun, D., Ramos, A. M., Ridder, N. N., Thiery, W., and Vignotto, E.: A typology of
compound weather and climate events, Nat. Rev. Earth Environ. 2020 17, 1, 333–347, https://doi.org/10.1038/s43017-020-
0060-z, 2020.